catalysts

MDPI

Article

Coke Characterization and Re-Activation Energy Dynamics of Spent FCC Catalyst in the Catalytic Pyrolysis of Polyolefins

Hussam A. Bahlouli, Rasha Alghamdi and George Manos *

Department of Chemical Engineering, University College London, Torrington Place, London WC1E 7JE, UK; hussam.bahlouli.22@ucl.ac.uk (H.A.B.); rasha.alghamdi.21@ucl.ac.uk (R.A.)
* Correspondence: g.manos@ucl.ac.uk; Tel.: +44-(0)-20-7679-3810

Abstract

Chemical recycling via catalytic pyrolysis is constrained by coke deposition and costly catalyst make-up. We investigate polypropylene (PP) and low-density polyethylene (LDPE) conversion over a spent FCC equilibrium catalyst (AXL) and, critically, quantify the re-activation energy landscape of the resulting coke. Using a semi-batch reactor (350 °C) and thermogravimetric analysis to 1100 °C combined with the Ozawa–Flynn–Wall method, we distinguish soft and hard coke under inert, oxidative, and sequential N_2 to air regimes. LDPE yields mainly gas (70.7 wt%) with 5.5 wt% coke, whereas PP favors liquids (47.1 wt%) with 3.4 wt% coke. LDPE-derived coke is softer (71% of total; E_A = 170 kJ mol^{-1} soft) than PP coke (60% soft; E_A = 166 kJ mol^{-1}), evidencing a more refractory PP residue. Oxygen lowers E_A to ~155 kJ mol^{-1} for both polymers. We introduce a simple TGA-based "softness ratio" to guide regeneration severity and show that a refinery-waste FCC catalyst delivers selective plastic-to-fuel conversion while enabling energy-aware regeneration protocols. The framework directly supports scale-up by linking polymer structure, coke quality, and atmosphere-dependent re-activation energetics.

Keywords: pyrolysis; heterogeneous catalysis; Zeolites; Polyolefins; recycling; coke characterization

Academic Editors: Soheil Valizadeh and Penglei Chen

Received: 24 July 2025
Revised: 5 September 2025
Accepted: 5 September 2025
Published: 6 September 2025

Citation: Bahlouli, H.A.; Alghamdi, R.; Manos, G. Coke Characterization and Re-Activation Energy Dynamics of Spent FCC Catalyst in the Catalytic Pyrolysis of Polyolefins. *Catalysts* **2025**, *15*, 862. https://doi.org/10.3390/catal15090862

1. Introduction

Polymer science, a core area of modern materials science, focuses on the study and application of macromolecules with complex structures and diverse functions. Polymers are central to modern life, serving as the building blocks for products ranging from everyday consumer goods to advanced medical and engineering materials. Among them, plastics, a group of synthetic polymers, are particularly valued for their versatility and low cost, enabling them to replace conventional materials in a wide range of applications [1]. The rapid growth in plastic production has raised serious global concerns about waste accumulation and its long-term environmental impact. Plastic pollution now poses a significant challenge to both terrestrial and marine ecosystems. Because plastics are resistant to natural degradation, they may last for centuries and harm wildlife, while posing potential threats to human health [2]. Microplastics, formed when larger plastic objects fragment into smaller pieces, are particularly hazardous. Microplastics can enter the food chain and accumulate in living organisms, creating further ecological and health concerns [3].

Global plastic production has exceeded 8300 million tons, much of which has been landfilled or discarded into the environment as long-term pollutants [4]. Plastic production

has increased sharply in recent decades, from about 275 million tons in 2010 to approximately 352 million tons in 2021 [5–7]. This steep rise is mainly due to the vast use of polymers, mostly plastics, in nearly all prominent economic sectors such as packaging, automobiles, and building construction. In response to the mounting environmental and waste management pressures, depolymerization has emerged as a central strategy for the recycling and treatment of polymer waste. The European Commission has also issued a goal for all plastic packaging becoming recyclable by 2030, part of broader initiatives toward reducing the environmental cost of plastic production expansion [8,9]. One key principle of sustainable waste management is the Waste Management Hierarchy, as described in the AXIL waste management framework. This supports waste prevention as the preferred approach, followed by reuse, recycling, recovery, and ultimately disposal as a last resort [10,11]. On a global scale, a small percentage of plastic waste is recycled annually, and there are great variations across regions in rates of recycling. Europe and India show comparatively high recycling rates, largely due to their well-developed waste management infrastructure and supportive policy measures [4,12,13].

The recycling rates among plastics differ considerably depending upon their categories. Low-density polyethylene (LDPE) is usually recycled into plastic bags, trays, and agricultural films, but LDPE recycling is still constrained by contamination problems and technological requirements for advanced sorting facilities [12]. Polypropylene (PP) is recycled into auto parts, textiles, and industrial products. However, its recycling remains limited by contamination and inefficient collection networks [7].

Chemical recycling, or advanced recycling, is a growing and innovative approach for plastic waste management that will supplement traditional mechanical recycling. While mechanical recycling reprocesses plastic mechanically into new raw material, chemical recycling disassembles plastic waste into its elemental chemical building blocks. This treatment allows for virgin-grade polymers and other useful chemical products, including from highly contaminated or degraded waste streams, to be produced. There are various important technologies involved in chemical recycling, each working through different mechanisms and producing different outputs. Thermal (non-catalytic) pyrolysis, also known as thermal cracking, is one of the most widely studied and applied processes in chemical recycling. The thermal decomposition of plastic waste under an oxygen-free condition results in a blend of liquid hydrocarbons, non-condensable gases, and solid residues (char) [14–16].Catalytic pyrolysis or catalytic cracking is the thermal decomposition of polymers in the presence of a catalyst, such as fluid catalytic cracking (FCC) catalysts, which enables the cleavage of long chain molecules into smaller, high-value-added hydrocarbons at much lower temperatures compared to thermal pyrolysis. The use of catalysts not only lowers energy requirements but also enhances product selectivity and improves yields of desired outputs. It provides improved control of product composition, which allows for customized production of light olefins, aromatics, or liquid fuels based on catalyst type and reaction conditions. Catalytic pyrolysis is found to have a high Technology Readiness Level (TRL) and is moving forward steadily towards commercial-scale deployment [16,17].

Modern FCC catalysts are hierarchical composite particles, typically 50–100 μm in diameter. These are formulated to maximize activity, selectivity, and deactivation resistance against hostile conditions experienced in catalytic cracking. They are composed structurally by Y zeolite crystals, often ultra-stable Y (USY), which are embedded in an amorphous silica–alumina matrix, supplemented by binder and filler additives assuring physical integrity and serving to form the catalysts [18–20]. A typical FCC catalyst contains about 15–40 wt% Y-zeolite, with the remaining 60–85 wt% comprising binder, filler, and matrix materials [18–20]. Every component plays a unique and critical role in formulating the FCC catalyst.

Fresh FCC catalyst differs substantially from a corresponding equilibrium catalyst (E-Cat) removed from an FCC unit after numerous cycles. Fresh FCC pellets contain well-crystalline USY zeolite with maximal acid site density [21]. E-Cat, however, exhibits lower activity and reduced zeolite concentration due to partial collapse of the zeolite to amorphous alumina/silica. Additional characteristics include a higher matrix-to-zeolite ratio accompanied by increased porosity, the presence of metals that promote gas production, and residual coke deposits on the spent catalyst. Despite these changes, equilibrium catalysts often perform remarkably well in specific applications owing to their moderated acidity and matured pore structure. Consequently, E-Cat catalysts are frequently evaluated for plastic cracking due to their lower cost and tailored acidity. Several studies have observed that an E-Cat catalyst can display more stable performance and a lower tendency toward coking when processing plastic feeds compared with a highly active fresh catalyst [22,23]. Although heavy metal contaminants can promote additional coke formation, mild operating conditions and regeneration can mitigate this effect. Vollmer et al. proved that polyolefinic wastes can be readily converted to hydrocarbons through catalytic pyrolysis with E-Cat catalyst. Importantly, it has been found in their work that the E-Cat performed better than its new counterpart, producing greater amounts of desired liquid product and having less coke formation. The better performance of the equilibrium catalyst was explained by its moderated acidity and increased porosity, built over prolonged use in refinery conditions. These factors probably reduced the amount of polymer condensation on the catalyst surface, thus inhibiting the buildup of deactivating carbonaceous materials [23].

Products were usually categorized into gaseous, liquid and solid fractions. Liquid hydrocarbon distribution was analyzed by boiling point distribution using gas chromatography, while solid residues (coke) were quantified gravimetrically [24–28].

Thermogravimetric Analysis (TGA) represents an essential characterization method in materials science, widely applied to polymers, composites, metals, and ceramics. It enables the evaluation of material composition, thermal stability, and degradation kinetics. The basic premise of TGA consists of heating a sample at a steady rate while monitoring changes in the sample's mass as a function of temperature under a specified atmosphere which can either be inert (for instance, nitrogen or argon) or oxidative (for instance, air or oxygen) based on the application desired [29]. Through the measurement of the rate of decomposition or reaction at different temperatures and conditions, TGA provides kinetic information. This information is typically displayed on a thermogravimetric curve, where mass is plotted versus temperature or time. The resulting thermogram reveals key thermal events such as moisture loss, decomposition stages, and overall thermal resistance [29]. By analyzing onset and offset temperatures, peak degradation points, and mass loss profiles, it is possible to assess the material's thermal behavior, composition, and degradation pathways.

Coke (solid carbonaceous residue) is a concern in catalytic pyrolysis processes because it deactivates the acid sites. The amount and nature of coke depend on catalyst acidity and the extent of secondary reactions (like hydrogen transfer and aromatization). Coke is classified as either soft or hard, depending on the volatility of its constituents. Soft coke, made up of confined oligomers, is more volatile than hard coke, which consists of more developed carbonaceous structures, as described by Corma et al. [30,31].

This study investigates the catalytic pyrolysis of LDPE and PP over a spent FCC equilibrium catalyst (AXL), focusing on product yields, coke deposition, and regeneration behavior. Using TGA–OFW up to 1100 °C under inert, oxidative, and sequential N_2 to air conditions, the activation energy of soft and hard coke was quantified, and a TGA-derived softness ratio was proposed to guide regeneration severity. Results show that oxygen

lowers the coke removal activation energy for both polymers, while PP-derived hard coke exhibits higher values than LDPE under inert conditions, linking polymer structure to regeneration energetics. These findings provide regeneration-relevant metrics that extend understanding of coke removal kinetics and complement established knowledge on product distributions in catalytic pyrolysis.

2. Results and Discussion

Unlike previous studies on spent FCC catalysts that emphasized product distributions, aromatics formation, or autothermal oxidative operation [23,32]. The present work resolves soft vs. hard coke and determines their OFW activation energies under N_2, air, and sequential N_2 to air, thereby providing actionable regeneration metrics for spent FCC systems.

2.1. Effect of Reactant Type on Product Distribution in FCC-Catalyzed Pyrolysis

As illustrated in Figure 1, the yields of gaseous, liquid, and coke products from the catalytic pyrolysis of LDPE and PP over the AXL catalyst were measured under controlled conditions: a 2:1 polymer-to-catalyst ratio, an inert nitrogen atmosphere, and a reaction temperature of 350 °C and a reaction temperature of 350 °C with a total reaction time of 1 h (ramp + isothermal hold).

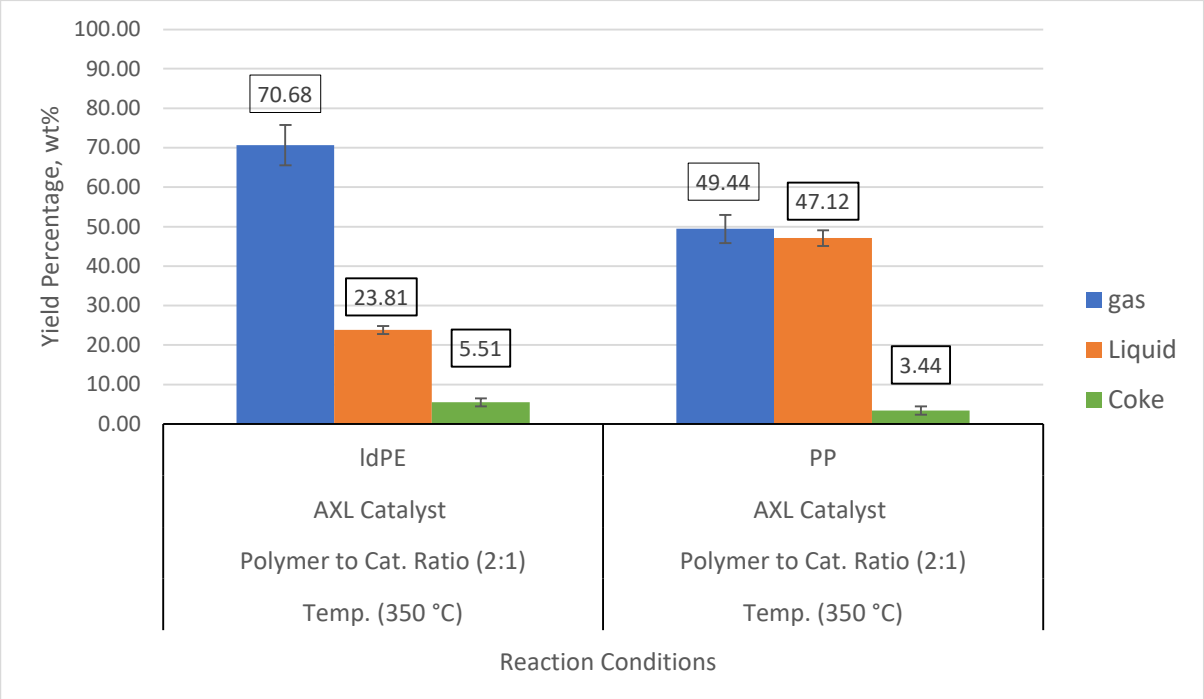

Figure 1. Comparison of gas, liquid, and coke yields from LDPE and PP pyrolysis using FCC catalyst at 350 °C.

All experiments were performed in triplicate ($n = 3$), and the reported values represent means with standard deviations: LDPE—gas 70.7 ± 8.0 wt%, liquid 23.8 ± 2.0 wt%, coke 5.5 ± 0.5 wt%; PP—gas 49.4 ± 4.0 wt%, liquid 47.1 ± 3.0 wt%, coke 3.4 ± 0.3 wt%.

Yields were calculated on a weight-percentage basis relative to the initial polymer mass, with the gas fraction determined by difference after quantifying the liquid and coke fractions (Equations (2)–(4) in Section 3). The gas fraction reported here represents permanent gases and light hydrocarbons up to C4. Heavier hydrocarbons (C5+) were condensed in the ice-bath condenser system and are included in the liquid fraction

Although 350 °C is lower than typical temperatures used in fluidized or spouted-bed catalytic pyrolysis, gas-dominated products at this setpoint are mechanistically consistent with semi-batch operation over USY-containing FCC under inert atmosphere, where prolonged vapor–catalyst contact, and strong external acidity promote secondary cracking. Prior semi-batch study over USY showed rapid formation of light C3–C5 gases and effective catalytic degradation at temperatures well below purely thermal limits [33]. Conversely, semi-batch vacuum operation at 370–430 °C over FCC/aluminum- pillared clay (Al-PILC) tends to be liquid-rich because reduced vapor residence suppresses secondary cracking [34]. Together, these comparisons support our observation that, at 350 °C, the combination of FCC acidity/metal function, atmospheric pressure, and long residence time can drive toward gas-rich products.

For LDPE, the product distribution was dominated by gaseous hydrocarbons, accompanied by moderate liquid formation and comparatively low coke deposition. This behavior reflects the strong tendency of LDPE to undergo extensive chain scission, yielding mainly lighter hydrocarbons with only a small amount of carbonaceous residue. However, additional factors such as secondary cracking/aromatization and diffusion within the FCC pore network also contribute to the high gas fraction. In contrast, PP exhibited a higher proportion of liquid hydrocarbons relative to LDPE, indicating a greater conversion efficiency into condensable products. Taken together, product distributions arise from the combined influence of polymer structure, secondary chemistry on acid sites, and transport within the FCC pore system, rather than a single molecular feature. Although PP also produced a substantial gas fraction, it was lower than that obtained from LDPE pyrolysis. Importantly, the coke yield from PP was reduced (≈3.4 wt%), suggesting a lower tendency for solid carbon deposition during reaction over the porous AXL catalyst.

These findings highlight the importance of polymer structure in influencing the yield of pyrolysis products. PP indicates a greater tendency for producing liquid hydrocarbons, while LDPE forms a higher percentage of gaseous product and coke. This difference in coke yield reflects variations in the thermal degradation behavior and molecular stability of LDPE and PP under comparable catalytic conditions. LDPE chains are less bulky, consisting mainly of secondary carbon atoms, whereas PP contains a methyl group on each repeating unit, creating tertiary carbon centers [35]. This structural difference makes PP less thermally stable and more susceptible to cracking than LDPE [36]. However, the methyl branches in PP promote the formation of bulkier fragments, which reflects not only the stabilizing effect of methyl-substituted intermediates but also diffusion constraints and stronger condensation pathways within the spent catalyst matrix. This inhibits further cracking and accounts for the relatively higher yield of liquid product found with PP [36–39]. LDPE, on the other hand, breaks down into linear fragments that more readily diffuse into the pores of the catalyst, facilitating further cracking and the production of lower molecular weight hydrocarbons which accounts for the higher yield of gas produced during the pyrolysis [36,39], or promoting recombination into longer chains, producing heavy oligomers or tar. When such recombination occurs near the catalyst's exterior pores, it contributes to coke formation [36–38].

It is well documented that USY zeolite, a key component of commercial FCC catalysts, significantly enhances product yield and reduces the required reaction temperature compared with thermal pyrolysis of LDPE and PP [40–42]. Moreover, USY has been found to be superior to other catalysts in terms of liquid fuel yield [43–45], which has been credited to the large supercages of USY in accommodating large hydrocarbon intermediates. The mesoporosity of the FCC catalyst facilitates access of LDPE and PP fragments to acid sites, enabling conversion while minimizing coke formation compared with other catalysts. This is partly attributed to the FCC catalyst composition, where the non-zeolitic components

control overall acidity and catalytic functionality to some extent [18–20,22,23,46]. In fact, the straight-chain segments and chain ends of LDPE are more capable than the bulkier chains of PP of penetrating catalyst micropores and accessing stronger acidic sites, thereby facilitating their breakdown into smaller hydrocarbon fragments. The synergistic effects of the FCC catalyst's mesoporosity and moderate acidity, tailored by its compositional design, help reduce, to some extent, the likelihood of these intermediates becoming trapped and evolving into coke precursors. This effect is particularly significant when compared to more acidic and less porous catalyst systems [38,39,43].

2.2. Residual Coke Characterization and Activation Energy Analysis

Spent catalysts from the catalytic pyrolysis reactions using AXL were collected and subjected to thermogravimetric (TG) analysis for coke characterization and determination of the activation energy for coke volatilization or oxidation.

2.2.1. Effect of Gas Atmosphere on the Thermal Behavior of Solid Residues

Thermogravimetric analysis (TGA) plots in Figures 2 and 3 reveal the weight-loss behavior of solid residues of spent AXL catalysts after the pyrolysis of LDPE and PP over different gaseous conditions (nitrogen and/or air) at a fixed rate of 5 °C/min. These analyses give information about the thermal stability and the decomposition pattern of the residues over specified temperature intervals. In the first stage, Zone A (25–200 °C), both LDPE- and PP-derived residues experienced minimal weight loss in all environments. Approximately 4 wt% of LDPE residue and 2.5 wt% of PP residue result from evaporation of moisture and volatile components. This regime was observed in both inert (nitrogen, orange and green curves) and oxidative (air, blue curve) atmospheres. The results show no significant decomposition during this range, an indication of the thermal stability of the residues at low temperature. The weight remains stable to around 210 °C in the inert conditions, whereas under oxidative conditions, stability to around 245 °C indicates a higher activation energy requirement for oxygen-induced decomposition.

In Zone B (200–600 °C), a slow weight reduction occurs in inert conditions. About 4 wt% of the weight loss represents the volatilization of soft coke in the case of LDPE derived residues, whereas in the case of PP derived residues, a smaller soft coke loss of about 2 wt% occurs. This indicates a relatively larger yield of soft coke by LDPE compared to PP pyrolysis. As the temperature nears the end of Zone B, the weight reduction stabilizes reflecting the near-entire elimination of soft coke in the inert conditions. Hard coke, however, became evident above 600 °C, particularly in the nitrogen atmosphere (orange curve). This reflects the thermal stability of this type of carbonaceous residue.

Introduction of air at 600 °C (green line) in Zone C resulted in a steep weight loss of about 2 wt% for both LDPE- and PP-derived residues, reflecting the sequential two-stage process. Soft coke is eliminated during the first inert heat treatment, whereas the oxidative atmosphere facilitates rapid breakdown of the remaining hard coke. This behavior reflects the vital role of oxygen in accelerating combustion reactions and promoting the breakdown of more stable carbonaceous components in the residues. After 800 °C in Zone D, very high temperatures or air are required to decompose and burn away the remaining hard coke. This reflects the limitations of inert atmospheres in total breakdown of coke deposits and the efficacy of the oxidative atmosphere in catalyst regeneration.

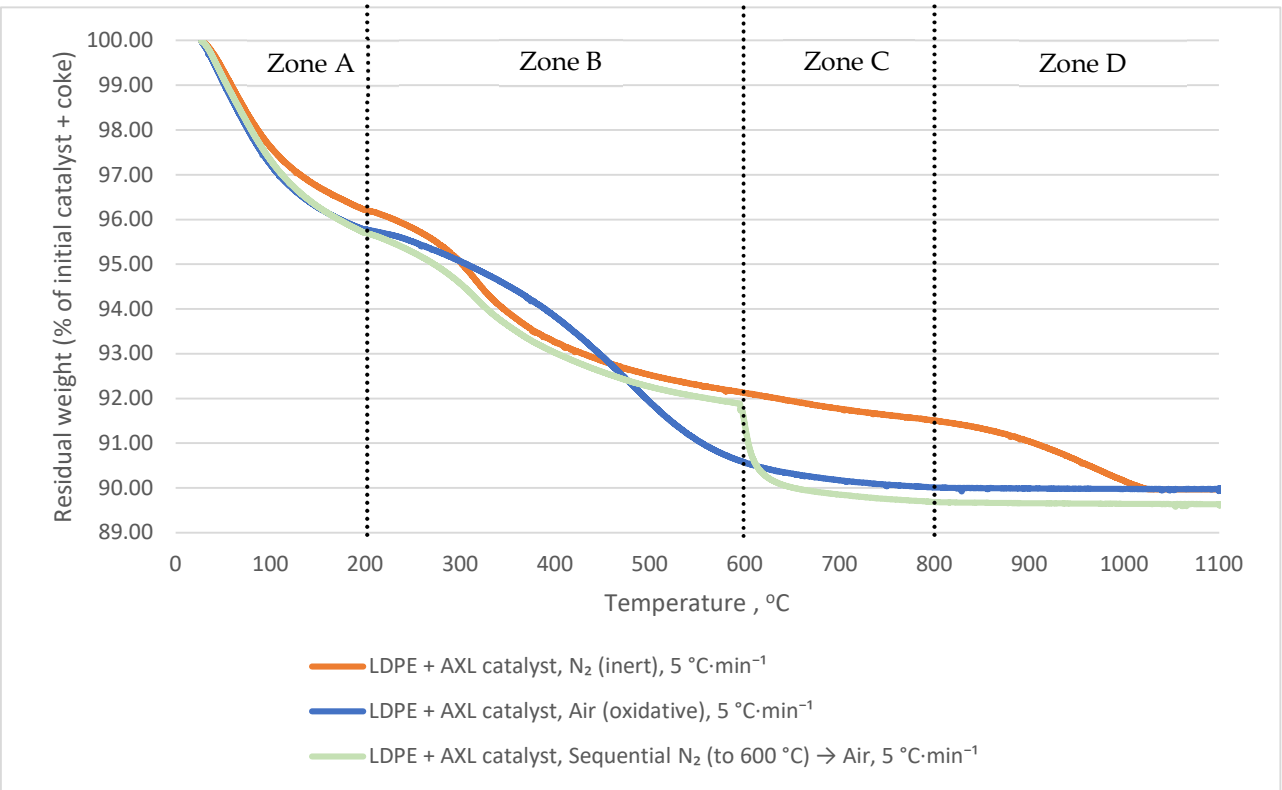

Figure 2. TGA weight-loss profiles of LDPE + AXL catalyst residues at 5 °C·min^{-1} under different atmospheres: N_2 only, air only, and sequential N_2 (to 600 °C) then air. The Y-axis represents the residual mass of the sample normalized to its initial weight.

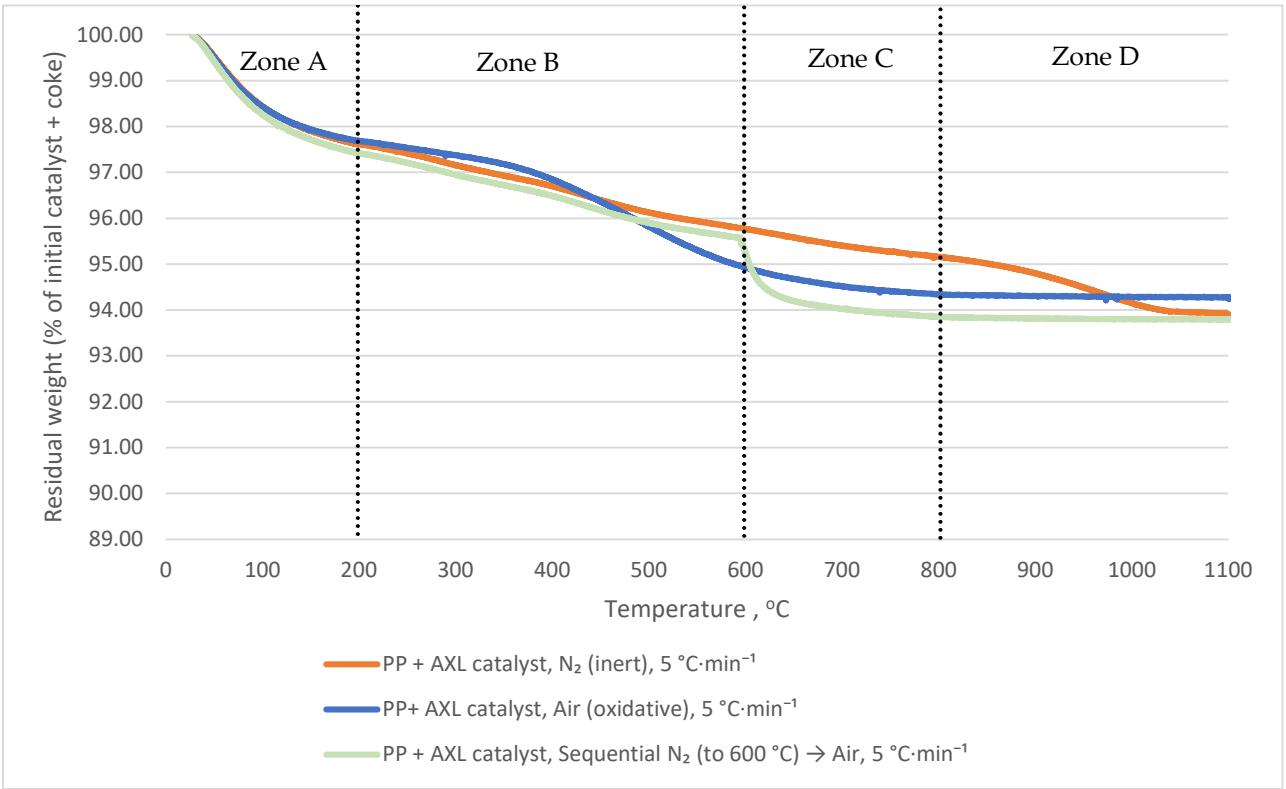

Figure 3. TGA weight-loss profiles of PP + AXL catalyst residues at 5 °C·min^{-1} under different atmospheres: N_2 only, air only, and sequential N_2 (to 600 °C) then air. The Y-axis represents the residual mass of the sample normalized to its initial weight.

Further differences can be seen with an air-only atmosphere (blue line), at which point major weight reduction occurs at around 245 °C. The oxidizing environment promotes the breakdown, meaning a total weight loss of around 6 wt% for LDPE residue and around 4 wt% for PP. This behavior indicates the enhanced capability of the oxygen atmosphere over inert conditions to eliminate both the soft and the hard coke depositions.

These experiments, performed at various heating rates (5, 10, 15, and 20 °C/min), provided vital information on the activation energy required to decompose coke under different gaseous conditions. A comparison of LDPE- and PP-based residues reveals different thermal behaviors, which are valuable to aid in the pyrolysis process optimization. These results are therefore vital to enhance the catalyst regeneration systems and for the control of carbon residues in industrial processes.

2.2.2. Influence of Polymer Type on the Thermal Decomposition of Solid Residues

Thermogravimetric analysis (TGA) results presented in Figure 4 characterize the weight loss behavior of solid residues from spent AXL catalysts after catalytic pyrolysis of LDPE and PP. The analysis was carried out in a sequential atmosphere of nitrogen and air under a constant 5 °C/min heating to 1100 °C and sheds light on thermal stability and decomposition dynamics through defined temperature zones. As shown in Figure 5, minimal weight loss occurred in Zone A (between 25 and 200 °C), a weight loss of around 4 wt% and 2.5 wt% for the LDPE and PP residues, respectively, corresponding to moisture and volatile compounds evaporation, in accordance with established findings in similar pyrolysis studies [31,47]. These small losses highlight the thermal stability of the residues under low temperatures in the presence of nitrogen. Zone B (210–600 °C) is characterized by progressive removal of mass through the volatilization of soft coke, with approximately 4 wt% of the LDPE-derived residue and 2 wt% of the PP-derived residue being eliminated, reflecting differences in amount of soft coke formation by the polymer type. The plateau of mass loss towards the upper temperature limit of this zone indicated that the inert atmosphere was insufficient to decompose the residual hard coke. At Zone C (600–800 °C), the presence of air triggers a rapid weight loss of around 2 wt% for both residues, signaling the hard coke's oxidative combustion phase. This decline underscores a two-stage decomposition mechanism where inert preheating eliminates volatiles and oxygen access allows hard coke degradation. This behavior highlights the critical role of oxygen in activating the decomposition of heavier carbonaceous materials. Zone D is the ultimate stable weight, which corresponds to the regenerated catalyst after removing nearly all of the residual by-products. Zone D represents the catalyst's preserved structure, which reflects its reusability after oxidation. These results also revealed differences in the activation energy of coke from LDPE and PP, based on TGA tests conducted at heating rates of 5, 10, 15, and 20 °C/min using the Ozawa method. Overall, the thermal analysis confirms the intricate nature of polymer type, atmosphere, and catalyst–coke influences and so gives valuable guidance to the optimization of catalytic pyrolysis.

The bar chart of Figure 5 displays a detailed compositional breakdown of solid residues produced on the catalytic pyrolysis of LDPE and PP over the AXL catalyst. It displays the amount of moisture and volatiles, soft coke, hard coke, and regenerated catalyst, offering valuable information on the thermal degradation behavior of each of the polymers' residues and the consequences of catalyst regeneration. A noticeable observation is the overall yield of coke of the two polymers' remnants. For LDPE, the combined yield of hard and soft coke equals approximately 5.9 wt%, of which 4.2 wt% exists in the form of soft coke and 1.7 wt% in the form of hard coke. For the PP sample, there is a smaller overall yield of 3.7 wt% consisting of 2.2 wt% soft coke and 1.5 wt% hard coke. These figures show that LDPE produces a greater amount of coke overall. Both polymers, however, exhibit a

higher proportion of soft coke relative to hard coke, reflecting their distinct decomposition behavior over the AXL catalyst. This outcome is attributed to the catalyst's mesoporous structure and moderated acidity.

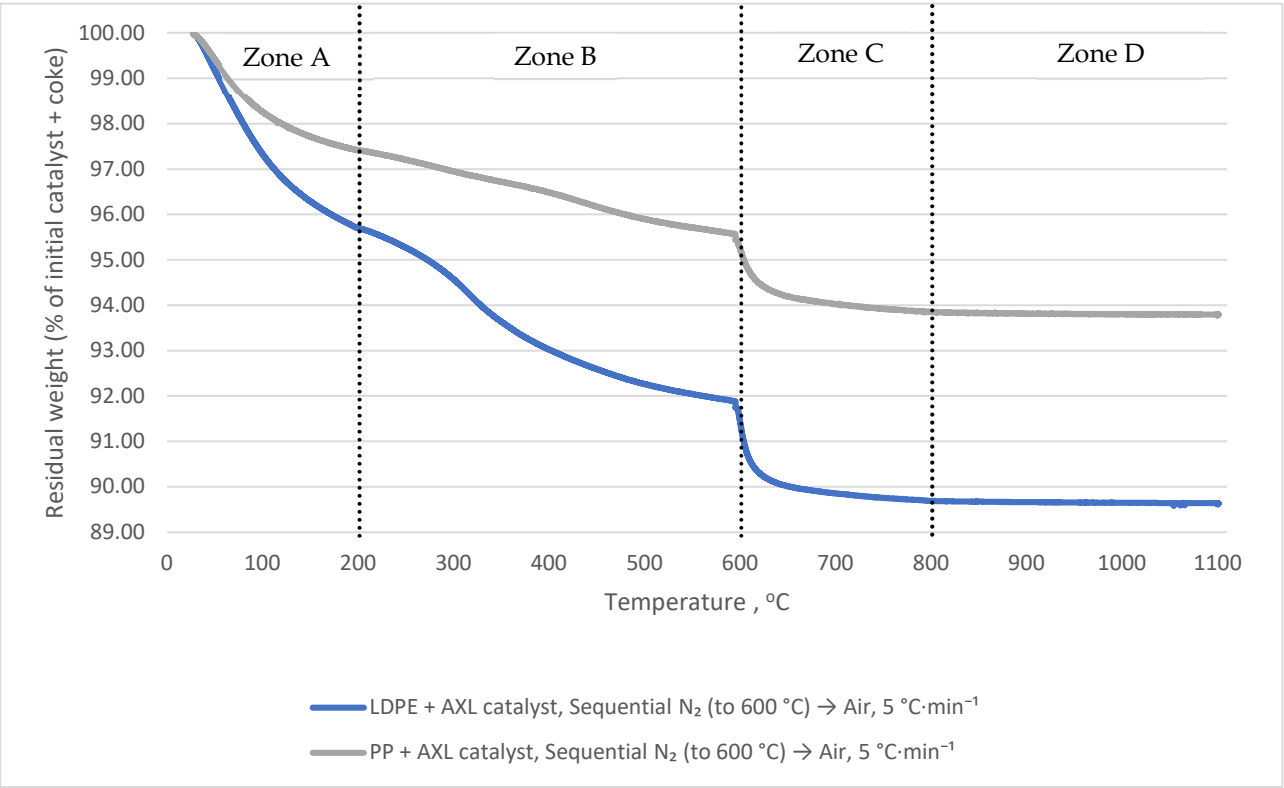

Figure 4. TGA weight-loss profiles of PP + AXL catalyst and LDPE + AXL catalyst residues at 5 °C·min^{-1} under sequential N_2 (to 600 °C) then air. The Y-axis represents residual sample mass normalized to its initial value. Weight decreases correspond to volatilization of soft coke (200–600 °C) and combustion of hard coke (>600 °C).

The degree of softness, which is one of the key indicators of coke properties, emphasizes the difference between the two polymers' residues. For LDPE, around 71% of the whole coke is recognized to be soft coke, reflecting a softer and looser residue that can easily be eliminated when regenerating catalysts. PP has a less softness ratio with just around 60% of its coke being classified as soft, reflecting the development of denser and tougher carbon deposits that are more recalcitrant to regeneration. In LDPE pyrolysis, heavy compounds build up on the catalyst surface and condense to form soft coke if not cracked to a large extent. In contrast to PP pyrolysis, which generates tertiary carbocations prone to β-scission, the resulting fragments are either small molecules or alkyl-aromatics that exit in the liquid part rather than accumulating as coke precursors [36]. This leads to fewer heavy residue deposits and inherently lowers soft coke formation. Additionally, secondary carbocations from LDPE are less prone to immediate scission and may undergo oligomerization or cyclisation on acid sites, leading to the formation of large multi-ring aromatics that contribute to soft coke accumulation [38,48]. For PP, the active and free strong acid sites of the USY zeolite component in the AXL catalyst are not occupied by heavy polyaromatic or polymeric species. As a consequence, there are PP-derived fragments that survive long enough to experience considerable polycondensation to form harder, graphitized carbon residues that accumulate deeper within the catalyst than those from LDPE fragments [36,49]. Such deeper deposition of PP-derived hard coke has direct implications for regeneration: being located in narrower pore channels and strongly condensed, it is

more resistant to oxidative removal and increases the risk of permanent loss of pore volume. In contrast, LDPE-derived coke, deposited closer to external surfaces, can be removed more completely, enabling more efficient recovery of catalytic activity.

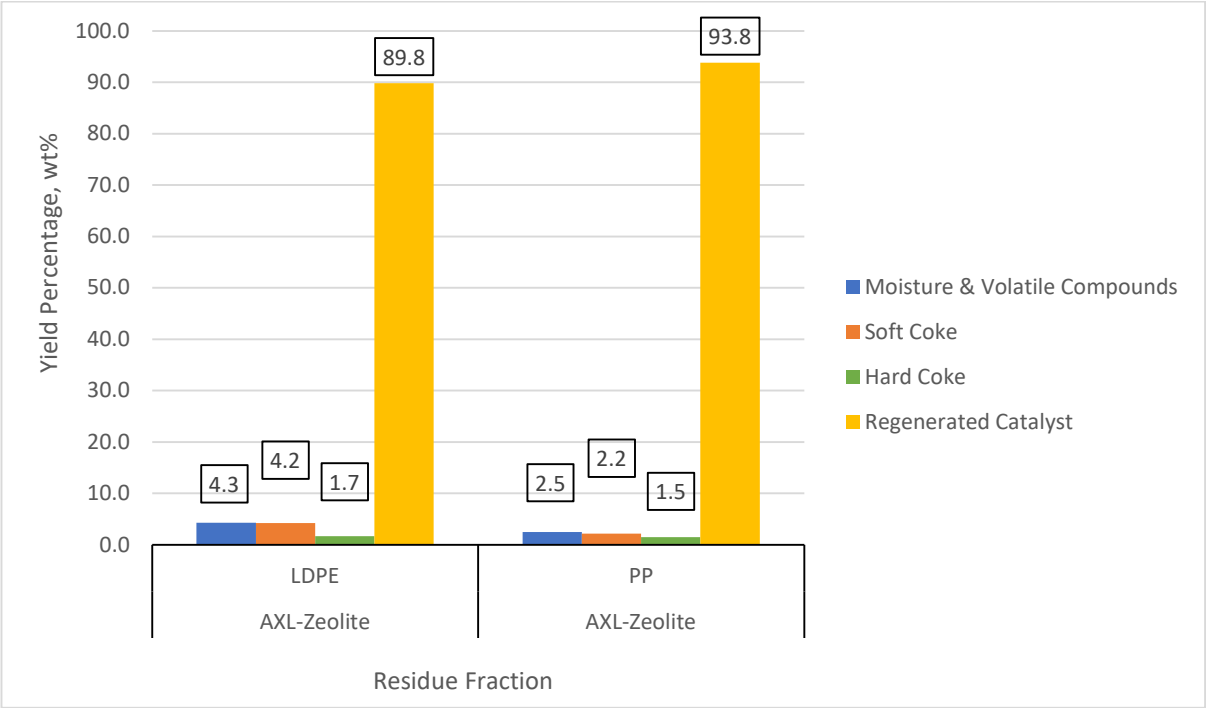

Figure 5. Compositional breakdown of solid residues from LDPE and PP pyrolysis over the AXL catalyst at 350 °C (polymer: catalyst = 2:1). Bars show moisture/volatiles, soft coke, hard coke, and regenerated catalyst fractions determined from TGA. LDPE residues contained 5.9 wt% total coke (4.2 wt% soft, 1.7 wt% hard), while PP residues contained 3.7 wt% total coke (2.2 wt% soft, 1.5 wt% hard). Both polymers produced a higher proportion of soft coke relative to hard coke.

Implications of such variations are far-reaching. Soft coke, with its greater reactivity and lesser density, could prolong catalyst lifetime through the reduction of extreme conditions needed to remove it. The opposite applies to hard coke, which is not only stabler and less prone to degradation but also renders catalyst regeneration tougher and operationally less efficient. These findings shed greater light on the unique thermal degradation mechanisms of LDPE and PP, and on the properties of the corresponding coke. Such information can guide process optimization routines that seek to minimize coke generation and maximize catalyst reusability.

2.2.3. Activation Energy (E_A) of Coke Deposited on AXL Catalyst

Although the OFW method is standard, its application here is distinctive: we apply it to resolve the activation energies of soft and hard coke fractions under different gas atmospheres on a spent FCC catalyst. To our knowledge, this atmosphere-resolved kinetic mapping of coke fractions has not been reported previously and provides direct guidance for regeneration protocols. Based on Equation (15) derived in Section 3.3 Characterization of Coke, the following calculation was employed.

$$E_A = \left(The\ Gradient\ of\ linear\ regression\ (best fit\ line)\ of\ Log\ of\ Heating\ Rate\ vs \frac{1}{T}\ at\ specific\ coke\ mass\ percentage \right) \times \frac{R}{\mu} \quad (1)$$

where

$$R = The\ universal\ gas\ constant = 8.3145 \left(\frac{\mathrm{J}}{\mathrm{mol} \times \mathrm{K}} \right)$$

$$\mu = Constant\ estimated\ by\ Doyle's\ approximation = -0.4567$$

By combining this calculation with the information given in the above sections, two sets of graphical charts have been plotted. The figures present the performance of coke deposits from spent AXL catalysts obtained from the catalytic LDPE and PP pyrolysis under different gaseous atmospheres:

Figures A1–A6 (see Appendix A) present the Ozawa–Flynn–Wall (OFW) plots, where log(Heating Rate/(°C·min^{-1})) is plotted against 1/T (K^{-1}) for LDPE- and PP-derived coke under N_2, air, and sequential N_2 to air conditions. Although reaction temperatures were set in °C, values were converted to Kelvin for kinetic analysis, as required by the Arrhenius relation. The slopes of the linear fits yield the activation energies (E_a) for soft and hard coke fractions.

Figures 6–9: Activation Energy vs. Coke Weight Remaining Percentage.

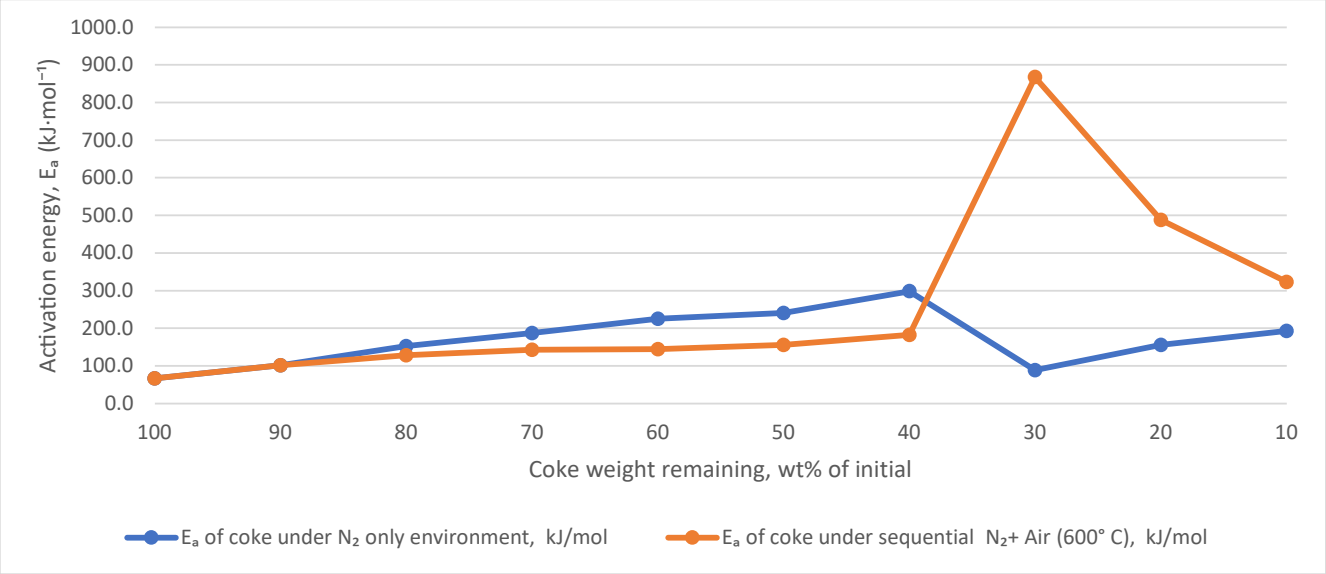

Figure 6. Activation energy (E_a, kJ·mol^{-1}) for LDPE-derived coke on AXL catalyst as a function of coke weight remaining (wt%). Results are shown for two gas environments: N_2 only and sequential N_2 (to 600 °C) → Air.

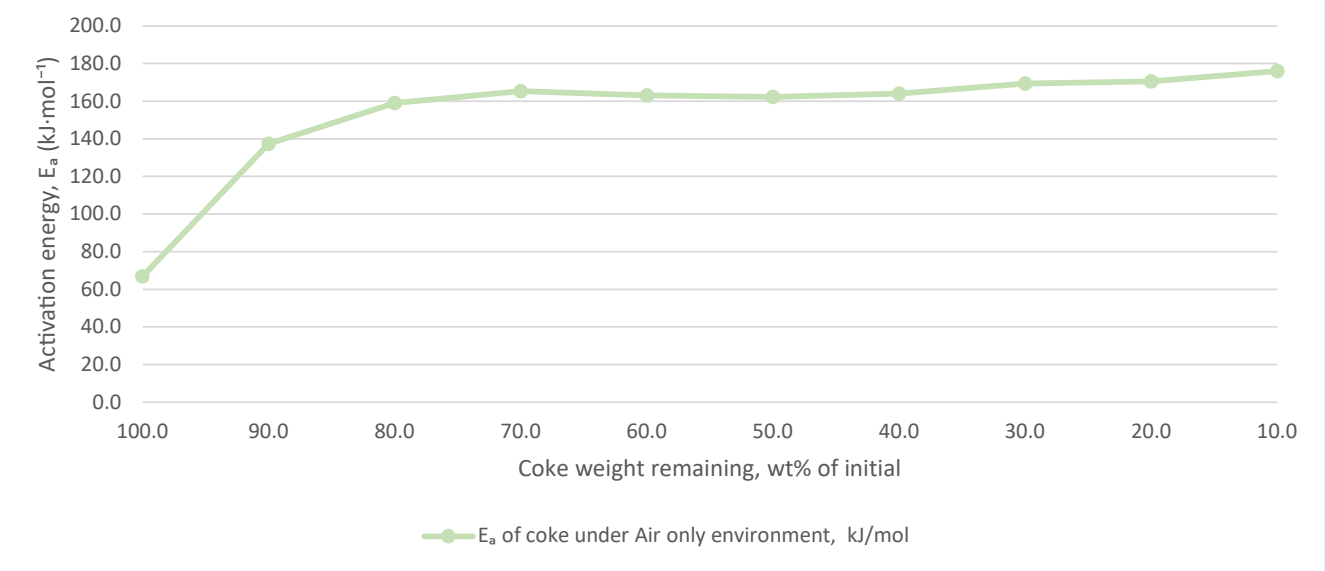

Figure 7. Activation energy (E_a, kJ·mol^{-1}) for LDPE-derived coke on AXL catalyst as a function of coke weight remaining (wt%), measured under air atmosphere.

Figure 8. Activation energy (E_a, kJ·mol^{-1}) for PP-derived coke on AXL catalyst as a function of coke weight remaining (wt%). Results are shown for two gas environments: N_2 only and sequential N_2 (to 600 °C) → Air.

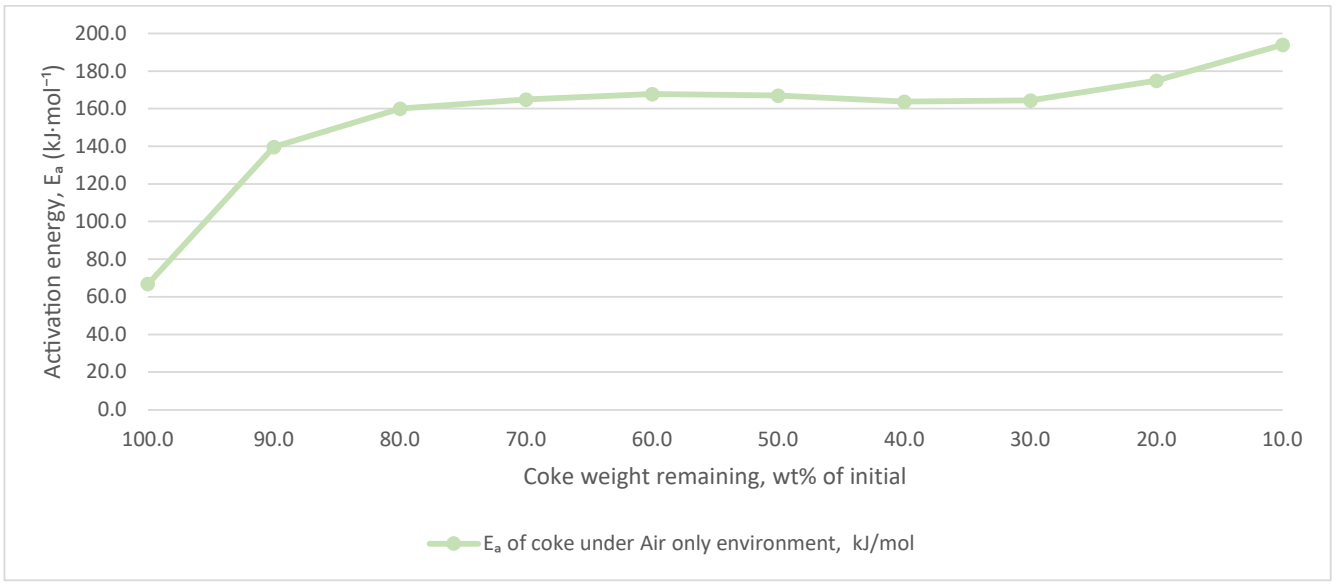

Figure 9. Activation energy (E_a, kJ·mol^{-1}) for PP-derived coke on AXL catalyst as a function of coke mass remaining (%), measured under air atmosphere.

The data analysis in Figures 6–9 is a critical analysis of the activation energy (E_A) required to strip coke deposits from spent AXL catalysts from the catalytic pyrolysis of LDPE and PP. The results highlight the effect of varying gas conditions (nitrogen, air, and a two-stage sequential nitrogen followed by air system) on the coke activation mechanisms. Notably, the results differentiate the energy requirements for hard and soft coke regions at different coke mass fractions, as atmospheric conditions change.

In a pure nitrogen environment (Figures 6 and 8), the decomposition dynamics clearly differentiate between soft coke and hard coke regions. With reference to studies conducted by Royo et al. and Luo et al., the observations for soft coke behavior under inert conditions align closely with prior findings in this study [50,51]. For the residues from LDPE pyrolysis (Figure 6, blue curve), the first region, up to 600 °C, corresponds to the removal of soft

coke and reflects 70% of the coke deposit mass. The average activation energy (E_A) in this phase is approximately 170 kJ/mol, with a notable decline in the curve indicating the total removal of soft coke achieved by volatilization. Beyond this phase, the transition into hard coke activation reveals an increase in energy demand, with an average activation energy (E_A) of 175 kJ/mol, reflecting the denser and more resilient composition of hard coke and emphasizing the energy-intensive of its decomposition in an inert environment. For residues from PP pyrolysis (Figure 8, blue curve), a similar trend is observed, but the soft coke phase accounts for 60% of the coke residue mass, indicating a lower proportion of soft coke compared to LDPE. The average activation energy for the soft coke phase is lower than what is observed for the residues from LDPE pyrolysis at 166 kJ/mol, and the average energy (E_A) for hard coke part is around 199 kJ/mol with the total (E_A) for both regions is 365 kJ/mol. These findings suggest that hard coke derived from PP requires more energy for activation and removal, correlating with its higher proportion. Notably, the degree of softness, a characteristic indicating ease of activation, is greater for coke residues from LDPE pyrolysis, as it requires less energy for both soft and hard coke activation taking the total amount of coke generated into consideration.

Under a sequential nitrogen-to-air (at 600 °C) environment (Figures 6 and 8, orange curves), the activation profile demonstrates different behavior. Soft coke is eliminated entirely by the end of the nitrogen phase, as seen by the low-energy requirement for the transition point shown by the blue curves. With the introduction of air environment, however, the activation energy surges dramatically, marking the oxidative degradation of the hard coke residues. This two-step behavior highlights the role of air in facilitating combustion reactions, which accelerates the breakdown of chemically stable coke residues. The energy contribution from combustion reactions influencing the process dynamics along with the pre-treatment with nitrogen changes composition and reactivity of the coke deposits, and the required energy goes down with decreasing mass of remnants. This is the reason why, in contrast to the pure nitrogen environment in which increasing coke hardness is accompanied by increasing energy requirements, the energy curves trend down as the coke hardness increases [50].

The comparative analysis of activation energies (E_a) across different environments highlights major differences in coke decomposition behavior. Under the present conditions (350 °C, 2:1 polymer-to-catalyst ratio, spent FCC catalyst), coke from LDPE pyrolysis required less energy for complete removal of both soft and hard fractions compared to coke from PP. This is consistent with the higher proportion of soft coke in LDPE residues, which is more reactive and readily oxidized. In contrast, PP generated a greater fraction of heavier, more resilient hard coke, demanding higher energy input for decomposition. It should be noted that the energy required for coke removal is also influenced by catalyst composition, temperature regime, and regeneration atmosphere.

Figures 7 and 9 present coke decomposition under the pure air atmosphere, where the differentiation between hard and soft coke becomes obscure. In contrast to an inert atmosphere, air triggers simultaneous combustion for all types of coke irrespective of the type of coke or its sources. For both LDPE- and PP-derived residues, the average activation energies were ≈155 kJ/mol, significantly lower than under pure nitrogen conditions. This reduction in energy reflects the exothermic character of oxidation, which activates coke in total at lower temperatures compared to the endothermic decomposition reactions in nitrogen atmosphere. However, during the late stages of hard coke combustion, there is a relatively small increase in the need for energy, probably a consequence of the greater resistance of highly condensed, stable carbonaceous material to oxidation [52].

These findings highlight the limitations of inert nitrogen environments, which, although capable of removing coke residues, require higher temperatures to activate hard

coke [53]. In contrast, our TGA and OFW results show that air atmospheres initiate coke removal at lower temperatures and with lower activation energies (~155 kJ·mol^{-1}) than under N_2 (166–199 kJ·mol^{-1}). This confirms experimentally that oxygen promotes combustion pathways which facilitate coke elimination more efficiently than purely thermal volatilization. Sequential nitrogen-to-air systems offer a strategic compromise, combining the thermal stability of inert phases with the oxidative efficiency of air, thus optimizing both coke decomposition and energy use.

Although the present work focuses on coke deposits rather than virgin polymer degradation, it is instructive to note that the activation energies measured here are of the same order of magnitude as those reported for LDPE pyrolysis in the absence of catalysts. For example, Dubdub and Al-Yaari reported ~193–195 kJ·mol^{-1} for non-catalytic LDPE pyrolysis under N_2 using iso-conversional methods [54], while Sinfrônio et al. observed a broader range of 126–275 kJ·mol^{-1} for LDPE and HDPE depending on the kinetic model applied [55]. In the case of coke decomposition, Al-Shathr et al. distinguished soft coke (90–118 kJ·mol^{-1}) and hard coke (140–203 kJ·mol^{-1}) on zeolitic catalysts [56]. Our results are consistent with these intervals but shifted upward: PP and LDPE-derived soft cokes required ~166–170 kJ·mol^{-1}, substantially higher than the 90–118 kJ·mol^{-1} reported for zeolitic soft coke, while PP-derived hard coke reached 199 kJ·mol^{-1}, lying at the upper bound of the 140–203 kJ·mol^{-1} range. This indicates that both 'soft' and 'hard' coke formed from polyolefin pyrolysis on a spent FCC catalyst are unusually condensed and refractory compared with coke typically observed on fresh zeolitic systems. Importantly, the sequential N_2 to air protocol revealed a distinct two-stage pathway, soft coke volatilization followed by hard coke oxidation, which, to our knowledge, has not been previously reported for FCC equilibrium catalysts.

This analysis highlights the relationship between gas atmosphere, coke type, and activation energy demand. It offers a clearer picture of thermal stability and decomposition, guiding improvements in catalyst regeneration and pyrolysis efficiency. By tailoring conditions to the nature of coke can reduce energy use and extend catalyst lifespan in industrial applications.

3. Methodology

3.1. Materials

PE (HMPE35A) and PP (HM20/70P) were purchased as fine white powders from Goonvean Fibres Ltd.,Cullompton, UK. The PE sample had an average particle diameter of 35 µm and a density of 0.91–0.92 g/cm^3, placing it within the LDPE range; it is therefore referred to as LDPE throughout this study. It has a melting point range of 98 °C to 113 °C. he PP sample had an average particle diameter of 90 µm, a density of 0.90–0.91 g/cm^3, and a melting point range of 159–171 °C [35,57–59].

The FCC catalyst used in this work, referred to as AXL and supplied by Aramco, Dhahran, Saudi Arabia, was a standard commercial composition. Typical commercial FCC catalysts contain around 15–40 wt% Y-type zeolite as an active part, the remaining 60–85 wt% of the composition consisting of binder, filler, and matrix materials, which collectively contribute mechanical strength, porosity, and support to catalytic action [18–20].

3.2. Semi-Batch Glass Reactor Rig

The experimental rig comprised a semi-batch Pyrex reactor(UCL Glass Workshop, London, UK) housed in a heating furnace, a PID temperature controller (Digi-Sense TC9600) (Oakton, Vernon Hills, IL, USA), two thermocouples (RS PRO, Beauvais, France), a PicoLog data acquisition system, and a gas supply line with a digital mass flow controller (Brooks Instrument, Hatfield, PA, USA) (Figure 10). The reactor (30 mm i.d., 35 mm o.d., 150 mm

height, 0.2 L volume) was fitted with two outlets, each connected to a pair of Pyrex condensers (UCL Glass Workshop, London, UK) immersed in an ice bath for liquid and condensable product recovery.

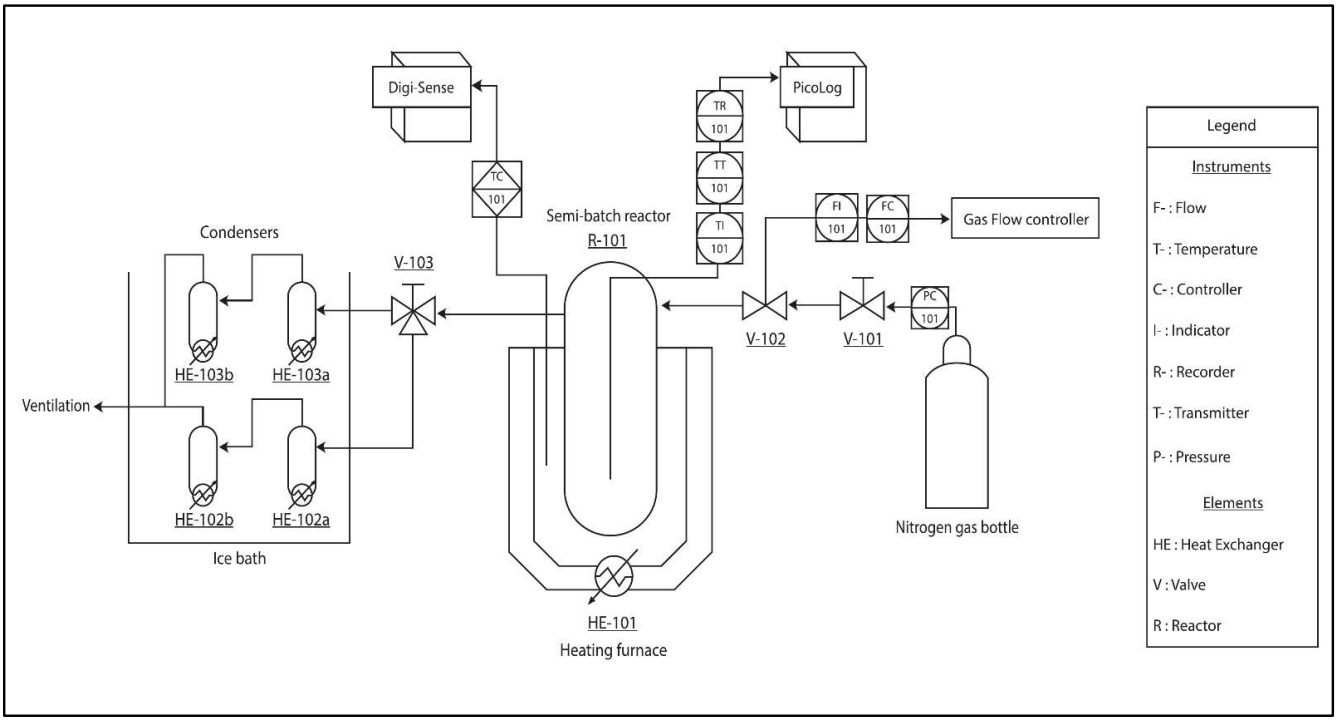

Figure 10. Process flow and instrumentation layout of the semi-batch Pyrex reactor system.

Heating was provided by two infrared elements regulated by a PID controller, with thermocouple TC101 (Type K) positioned between furnace and reactor for feedback control. Heating profiles, setpoints, and ramp rates were programmed digitally [60]. The internal reactor temperature was measured with thermocouple TR101 (Type K) linked to a Pico USB TC-08 logger, with real-time data acquisition and export via PicoLog software(V7.1.13) [61]. Nitrogen was supplied at 100 mL·min^{-1} and 1 bar (regulated by PC101 and FC101) (Swagelok Company, London, UK) and exited through one reactor outlet, carrying volatile products to the condensers.

All materials were inspected for contamination and dehydrated prior to use. Polymer and catalyst quantities were measured on a precision balance according to the prescribed ratio. Condensers and reactor were pre-weighed, then re-weighed after loading with the polymer–catalyst mixture to determine the dosed mass. The reactor was connected to condensers via flexible tubing and purged with N_2 for 15 min (PC-101, V-101, V-102 open) to stabilize the atmosphere. The furnace (HE-101) was raised into position, V-103 set to the selected condenser line, and ice added to ensure full submersion of the condensers. Under these conditions, all C5+ hydrocarbons were condensed and collected as liquid, while the gas fraction quantified here includes only permanent gases and light hydrocarbons up to C4 Following leak verification, PicoLog and Digi-Sense controllers were activated to monitor and regulate the programmed heating profile. The furnace was powered on to initiate the reaction, then switched off and lowered at completion. Software systems were shut down, and N_2 purging continued briefly before gas flow was stopped. For each experiment, the total reaction time was 1 h, comprising the programmed ramp to 350 °C and an isothermal hold at the setpoint. Post-reaction, the reactor, condensers, and tubing were dismantled and reweighed to determine liquid, gas, and coke yields (Equations (1)–(3)). Condensates and solid residues were collected in labeled vessels. The apparatus

was then cleaned and oven-drying at 550 °C for ≥30 min to ensure complete removal of contaminants before subsequent runs.

$$\text{Yield of Liquid Product}(\%) = \frac{\text{Weight of liquid collected in the Condensers}}{\text{Intial Polymer Weight}_{before\ reaction}} \times 100 \quad (2)$$

$$\text{Yield of Total Coke}(\%) = \frac{\text{Weight of Coke on Catalyst}}{\text{Intial Polymer Weight}_{before\ reaction}} \times 100 = \frac{\text{Difference between Weights of the Reactor \& Coked Catalyst at the end of experiment and Empty Reactor}}{\text{Intial Weight of the Polymer}_{before\ reaction}} \times 100 \quad (3)$$

$$\text{Yield of Gas Product}(\%) = 100 - (\text{Yield of Liquid Product} + \text{Yield of Total Coke}) \quad (4)$$

3.3. Characterization of Coke

Coke deposition in pyrolytic catalysis occurs in two major forms: soft coke and hard coke, each characterized by distinct physicochemical properties, regeneration behaviors, and effects on catalytic performance [47]. Table 1 provides a detailed comparison between soft and hard coke in the context of pyrolytic catalysis.

Table 1. Comparative Characteristics of Soft and Hard Coke in Pyrolytic Catalysis.

Aspect	Soft Coke (Volatile Coke)	Hard Coke (Refractory Coke)
Definition	loosely bound, thermally labile carbonaceous materials	graphitized, heavily condensed carbon residue
Composition	primarily aliphatics and lighter aromatics	highly polyaromatic structures
Location on Catalyst	found on both external and internal catalyst surfaces	deeply embedded in catalyst pores and strong acid sites
Thermal Stability	low thermal stability	high thermal stability
Regeneration and Impact on Catalyst	easily removed under mild oxidative conditions, with minimal structural damage and full recovery of activity	requires severe high-temperature or chemical regeneration, often leading to partial or irreversible catalyst degradation
Impact on Catalytic Performance	temporary deactivation; activity can be largely restored	causes long-term or irreversible deactivation by blocking active sites
Relevance in Plastic Pyrolysis	essential for optimizing regeneration and maintaining catalyst performance in sustainable recycling	crucial to control for extending catalyst life and ensuring stability in continuous or industrial pyrolysis applications

TGA was performed at the Centre for Nature-Inspired Engineering (CNIE) laboratory using a STARe System TGA/DSC 3+ (Mettler Toledo, Greifensee, Switzerland). The instrument is equipped with a high-performance furnace capable of reaching 1600 °C and a precision balance with 0.1 μg sensitivity for detecting minute mass changes. It supports operation under both inert (argon, nitrogen) and reactive (air) atmospheres with controllable

heating rates from 0.001 to 500 °C min^{-1}, and includes a chiller for efficient temperature regulation and rapid cooling. Data acquisition and processing were conducted using STARe software (V16.30), which provides kinetic evaluation, peak integration, baseline correction, and automated reporting.

In a typical TGA run, alumina crucibles were cleaned, rinsed with water and alcohol, oven-dried, and positioned on the autosampler arm. The software recorded the crucible tare weight before ~10 mg of solid residue from the catalytic pyrolysis reaction was loaded. The thermal program was then initiated, and mass loss profiles were collected for subsequent interpretation. Soft, hard, and total coke concentrations were determined from the respective mass losses, normalized to the final catalyst mass after complete coke removal, as described by Equations (5)–(7).

Soft coke includes all coke components volatilized, i.e., vaporized and/or decomposed to volatile species, in an inert nitrogen atmosphere. Besides quantifying the total soft coke, the TGA method used here also provides its distribution with temperature. Hard coke, on the other hand, comprises the remaining coke fractions that can only be removed in an oxidative atmosphere, i.e., through combustion. By combining both nitrogen and air environments in a sequential N_2 to air protocol, thermally labile soft-coke volatilization can be clearly distinguished from subsequent hard-coke oxidation under regeneration-relevant conditions.

$$\text{Concentration of Soft Coke} = \frac{\text{Mass of Soft Coke}}{\text{Mass of Catalyst}} \tag{5}$$

$$\text{Concentration of Hard Coke} = \frac{\text{Mass of Hard Coke}}{\text{Mass of Catalyst}} \tag{6}$$

$$\text{Concentration of Total Coke} = \frac{\text{Mass of Total Coke}}{\text{Mass of Catalyst}} \tag{7}$$

The Ozawa method can be employed to calculate the activation energy of the coke in the residues [47,62–65]. This method has the advantage of estimating the activation energy irrespective of the reaction rate, enabling comparisons to be made between catalysts and coke types generated on these catalysts. The method requires the collection of TGA information at several different rates of heating, taking the temperature corresponding to a specific conversion level at each rate. A plot of the decadic logarithms of the rates of heating against the reciprocals of the absolute temperatures generates straight lines. The gradient of each line is in direct proportion to the activation energy. The mean activation energy of coke removal is the result of averaging the values derived at various levels of conversion for the particular catalyst and coke sample.

Although catalytic cracking is a complex process, kinetic interpretation of TGA data commonly employs a simplified model in which the overall degradation rate (r) is described by a basic kinetic equation [47,62–65]:

$$r = -\frac{dw}{dt} = kw^n = Aexp\left(-\frac{E_A}{RT}\right)\cdot w^n \tag{8}$$

where r is the degradation rate, k is the reaction rate constant, w^n is the fractional residual weight which can be described as $w = 1 -$ converison, n is the reaction order, E_A is the activation energy, T is the absolute temperature, and R is the universal gas constant (8.314 J·mol^{-1}·K^{-1}).

During the TGA experiment, the temperature increases at a constant rate α, expressed as:

$$T = T_0 + \alpha\, t \tag{9}$$

Integrating the rate equation (Equation (9)) with Doyle's approximation:

$$\int_{w_0}^{w} -\frac{dw}{w^n} = \frac{A}{\alpha}\int_{T_0}^{T} exp(-\frac{E_A}{RT})dT = \frac{A}{\alpha}\cdot\frac{E_A}{RT}\cdot p(\frac{E_A}{RT}) \tag{10}$$

where p is a function whose decadic logarithm is estimated by Doyle:

$$logp\left(\frac{E_A}{RT}\right) = \lambda + \mu\left(\frac{E_A}{RT}\right) \tag{11}$$

with the constants λ and μ are found using Doyle's approximation. For our application μ is calculated to be equal -0.4567 .

For a specific fractional weight w, the left-hand side of the integrated equation (Equation 10) is constant and denoted as $F(w)$. By taking the decadic logarithms of the integrated equation (Equation (10)):

$$log(F(w)) = logA + logE_A - log(R) - log(\alpha) + \lambda + \mu\left(\frac{E_A}{RT}\right) \tag{12}$$

this equation (11) can be rewritten as:

$$\log(\alpha) = \upsilon + \mu\left(\frac{E_A}{RT}\right)\cdot\frac{1}{T} \tag{13}$$

where $\upsilon = logA + logE_A - log(R) - log(\alpha F(w)) + \lambda$.

Plotting $log(\alpha)$ against $\frac{1}{T}$ gives a linear graph with a slope of:

$$Gradient = \mu\cdot\left(\frac{E_A}{RT}\right) \tag{14}$$

Thus, activation energy E_A can be calculated as:

$$E_A = Gradient\cdot\left(\frac{R}{\mu}\right) \tag{15}$$

The procedure for determining the activation energy of coke on a specific catalyst is repeated for each fractional coke weight (w), corresponding to a particular conversion level. The activation energies estimated at various conversion levels are then averaged to represent the activation energy of the coke–catalyst system.

3.4. TG Temperature Program

Figure 11 displays an elaborate description of the temperature program used in TGA to characterize coke and to calculate the activation energy. The program has been divided into discrete regimes based on certain specified heating rates, conditions for the flow of the gases, and intervals of isothermal soaking.

First, the temperature ramps up uniformly at 2 °C/min to 200 °C at a controlled flow of 50 mL/min of either air or nitrogen (N_2). This first phase (black line) serves to efficiently eliminate moisture and adsorbed volatiles and sets the stage for subsequent analyses. The intermediate phase (blue line) takes the temperature through 200 °C to 600 °C at 5, 10, 15, and 20 °C/min variable rates, with the same flow of the gases. This stage focuses on volatilizing or decomposing of less stable components in the sample, particularly the soft coke. The final heat phase (orange line) raises the temperature to 1100 °C at the same variable heat rates, with the addition of a 120 min isothermal soak. This stage provides a measure of the thermal behavior and stability of more resilient materials like hard coke. The

controlled heat input and extended soaking period in the final stage ensures comprehensive capture of the thermal behavior and stability of these more resilient materials.

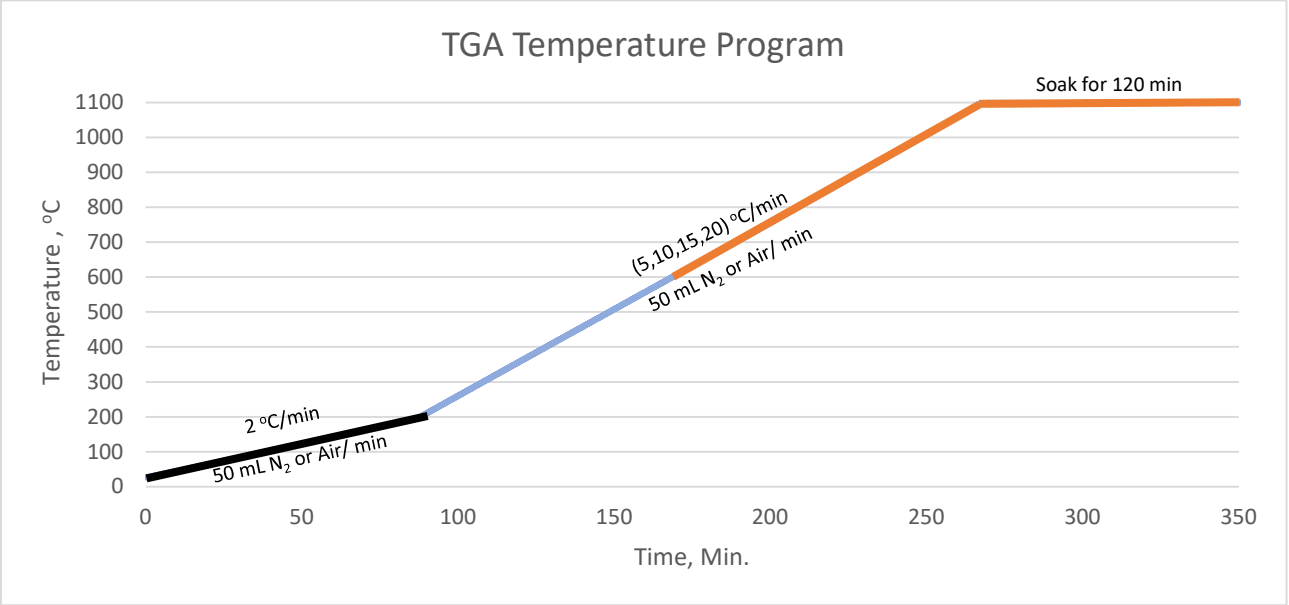

Figure 11. Stepwise TGA heating protocol for volatile removal and coke analysis.

This tailored temperature program allows for a thorough and detailed assessment of the thermal properties of coke. By observing its behavior across distinct thermal regimes, valuable insights into its composition and stability can be obtained, supporting accurate determination of activation energy.

4. Conclusions

This study critically examines the catalytic pyrolysis of PP and LDPE over AXL, a spent FCC catalyst, providing insights into product yields, residual coke behavior, and the energy dynamics of coke decomposition. Thermogravimetric analysis (TGA) was employed to characterize thermal degradation pathways, while the Ozawa–Flynn–Wall method was applied to determine activation energies. Using a TGA setup spanning 25–1100 °C, volatilization and oxidation processes were investigated in detail, establishing a robust framework for understanding coke behavior and catalyst interactions under varied thermal and atmospheric conditions. The results reveal clear differences between LDPE and PP during pyrolysis.

LDPE produced mainly gaseous product (70.7 wt%), with moderate liquid yield (23.8 wt%) and little coke formation (5.5 wt%), corresponding with its propensity toward breakdown into lighter hydrocarbons. This is attributed to LDPE's linear molecular structure, which favors extensive β-scission and random chain cleavage, leading to volatile hydrocarbons. In contrast, liquid and coke yields remain lower, as fewer stable condensable species are produced. In contrast, PP produced a higher liquid yield (47.1 wt%) with lower coke formation (3.4 wt%), indicating greater efficiency in liquid-phase product generation. These differences are closely linked to polymer structure, as the branched characteristic of PP promotes the formation of more stable, higher-molecular-weight olefinic and aromatic intermediates, which preferentially condense into liquid hydrocarbons rather than volatilize.

The small difference in activation energy between LDPE-derived soft coke (170 kJ·mol^{-1}) and hard coke (174 kJ·mol^{-1}) suggests that the deposits formed are comparatively homogeneous in structure. This behavior arises because LDPE's linear chains undergo extensive

random chain scission which produces less aromatic and more labile residues. Consequently, the boundary between soft and hard coke fractions is less pronounced, resulting in closely aligned activation energies. By contrast, PP-derived coke showed a clearer separation between soft (~166 kJ·mol^{-1}) and hard fractions (up to 199 kJ·mol^{-1}). The branched nature of PP chains stabilizes radical intermediates differently, favoring the formation of more condensed, aromatic species. These condensed structures accumulate as refractory hard coke, thereby widening the activation energy gap between soft and hard fractions. This contrast highlights how polymer structure directly governs not only overall coke yield but also the relative stability of coke fractions formed on a spent FCC catalyst. Overall, the contrast between LDPE and PP underscores the need for polymer-specific regeneration protocols: LDPE-derived coke can be targeted with milder, energy-saving oxidative treatments, while PP-derived coke requires harsher conditions or alternative regeneration strategies. Embedding such regeneration-aware metrics into process design could extend catalyst lifetime and lower costs in large-scale chemical recycling.

Under oxidative conditions, the activation energy requirement fell into the range of ~155 kJ·mol^{-1} for both polymers, reflecting the overall increased efficiency of coke oxidation. This behavior does not indicate greater coke stability in air; rather, it highlights that oxygen disrupts condensed heavy compounds and promotes combustion pathways, thereby lowering the apparent barrier to coke removal. This explains why oxidative regeneration is more energy-efficient than inert treatments and why oxygen availability is critical for complete elimination of refractory coke deposits.

The strength of the study lies in the coupling of controlled experimental design with sound analysis techniques. With a semi-batch glass reactor, it proved the effectiveness of the AXL catalyst in the conversion of LDPE and PP into more valuable hydrocarbon products. Its high mesoporosity, thermal stability, and moderate acid-site density contributed to its superior performance, making it a crucial material in the field of catalytic pyrolysis. Nevertheless, coke formation and catalyst deterioration are constraints that further stress the need for further advancement in catalyst formulation and regeneration methods.

With global plastic production exceeding 8300 million metric tons and recycling rates remaining below 10%, catalytic pyrolysis offers a sustainable pathway for converting waste into fuels and chemicals. By linking polymer structure, coke characteristics, and atmosphere-dependent regeneration energetics, this study establishes regeneration-focused metrics that complement existing knowledge on product distributions and inform the future scale-up of plastic-to-fuel technologies.

In this study, the operating conditions (350 °C, 2:1 polymer-to-catalyst ratio) were deliberately fixed to isolate coke behavior, allowing us to establish clear links between coke composition, catalyst performance, and process conditions during catalytic pyrolysis. The sequential nitrogen-to-air strategy proved particularly effective, exploiting inert conditions for soft coke volatilization and oxidative conditions for hard coke combustion, thereby generating regeneration-relevant metrics to guide catalyst reuse and process optimization. The contrasting product distributions of LDPE and PP further underline the importance of polymer structure in shaping coke quality, offering insights that can inform the treatment of mixed plastic waste streams. Building on this framework, future work will systematically explore the effects of temperature, catalyst loading, and feedstock composition on product selectivity, alongside the use of alternative TGA gas atmospheres. Of particular interest is CO_2, which will be investigated to assess whether a reverse Boudouard reaction occurs with carbonaceous coke. Comparative studies using fresh FCC catalysts and zeolite-based systems will also be pursued to evaluate how catalyst age, acidity, and porosity govern coke properties and regeneration dynamics. Finally, while gas and liquid yields were reported here as overall mass fractions to contextualize coke formation, forthcoming studies will

incorporate detailed chemical analyses (e.g., GC–MS of liquid products) to deliver a more comprehensive understanding of product distributions.

Author Contributions: Conceptualization, G.M.; methodology, G.M., H.A.B. and R.A.; software, H.A.B.; validation, G.M., H.A.B. and R.A.; formal analysis, G.M., H.A.B. and R.A.; investigation, G.M., H.A.B. and R.A.; resources, G.M.; data curation, G.M., H.A.B. and R.A.; writing—original draft preparation, H.A.B. and R.A.; writing—review and editing, G.M.; visualization, H.A.B.; supervision, G.M.; project administration, G.M.; funding acquisition, G.M. All authors have read and agreed to the published version of the manuscript.

Funding: This study was funded by Saudi Aramco. The support provided by Aramco enabled the resources and infrastructure necessary to conduct this research. The content presented in this publication is solely the responsibility of the authors and does not necessarily represent the views of Saudi Aramco.

Conflicts of Interest: The authors declare no conflict of interest.

Appendix A

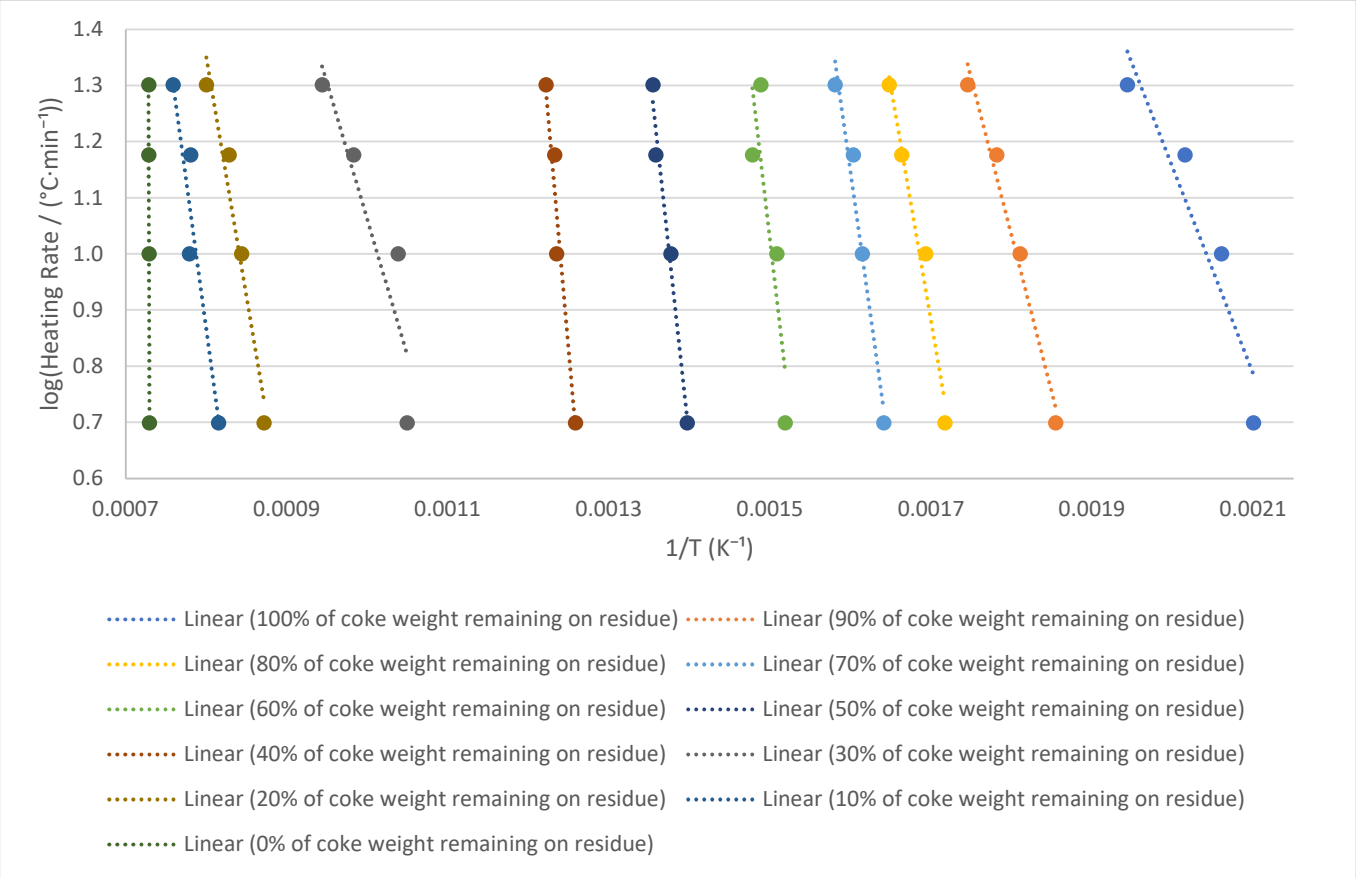

Figure A1. Ozawa–Flynn–Wall (OFW) plot for LDPE-derived coke on AXL catalyst under N_2 atmosphere. Y-axis: log(Heating Rate/(°C·min^{-1})); *X*-axis: 1/T (K^{-1}). Slopes of the linear regressions at different conversion levels provide activation energies (E_a) for coke volatilization.

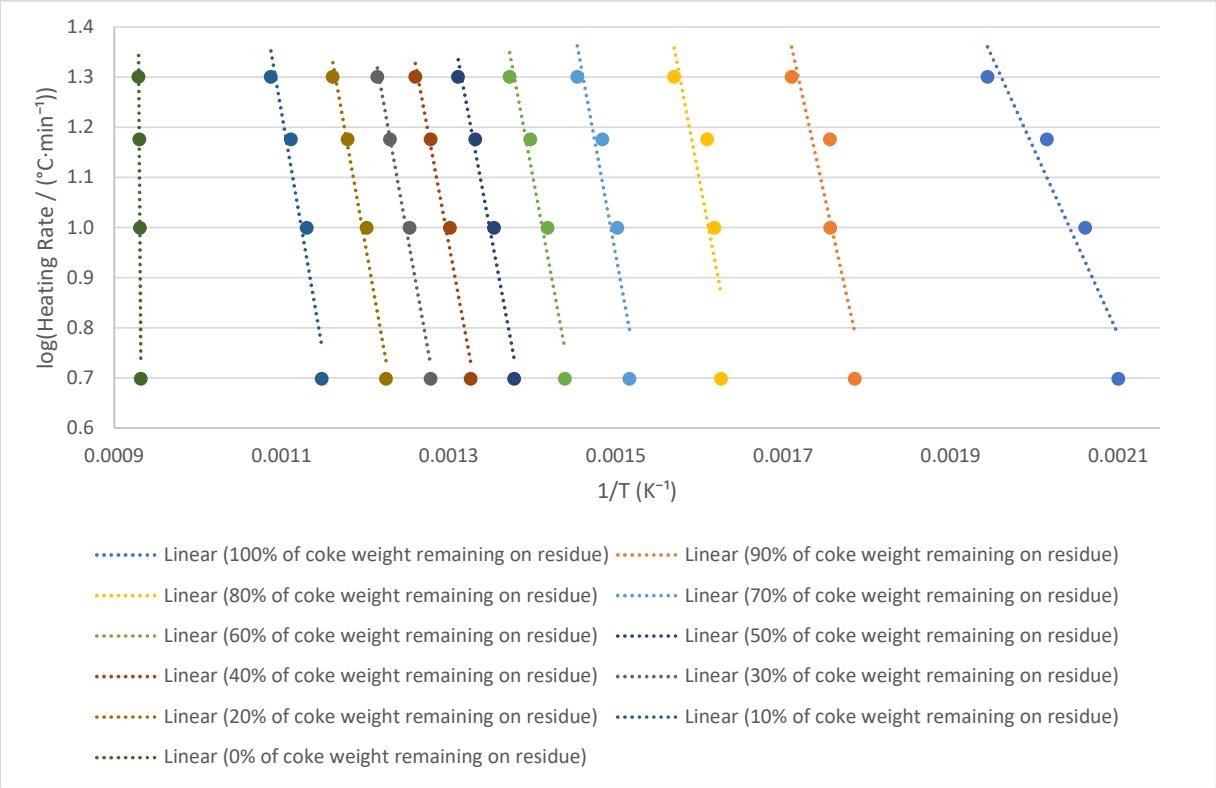

Figure A2. OFW plot for LDPE-derived coke on AXL catalyst under air atmosphere. Y-axis: log(Heating Rate/(°C·min^{-1})); *X*-axis: 1/T (K^{-1}). Activation energies determined from the slopes correspond to oxidative combustion of coke fractions.

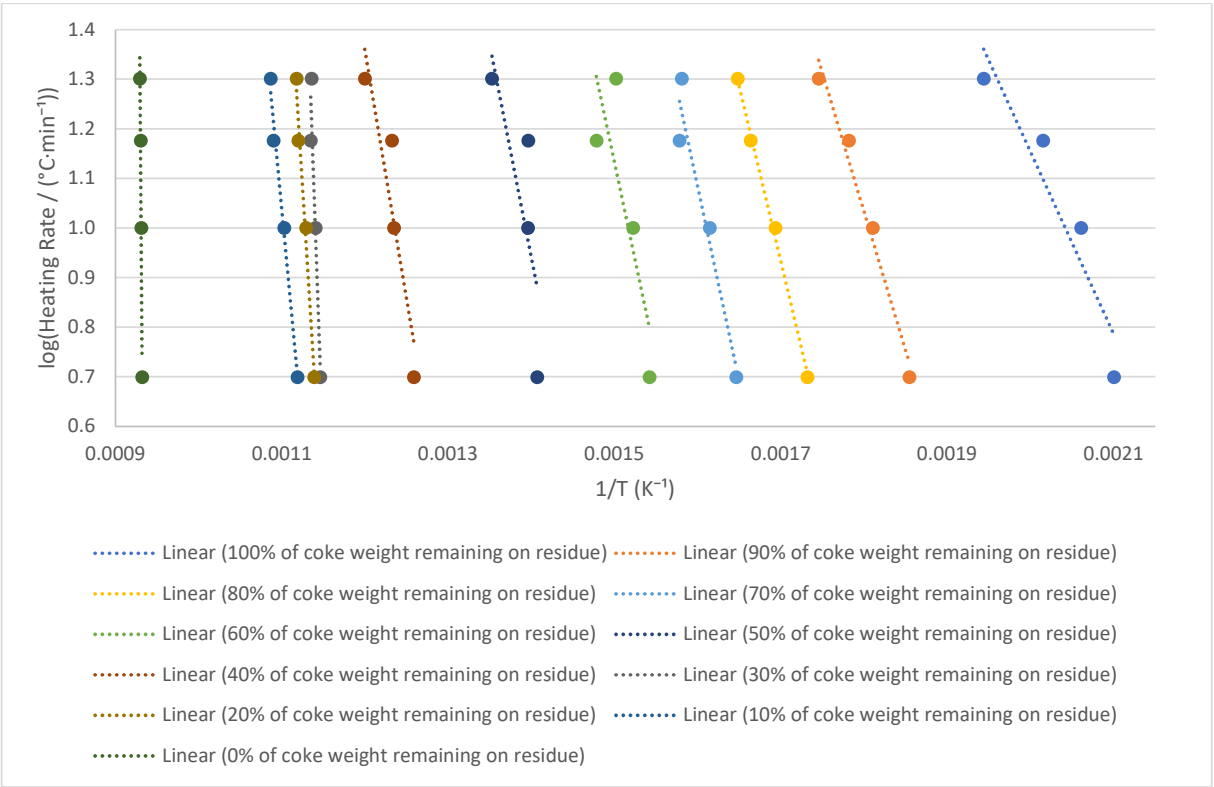

Figure A3. OFW plot for LDPE-derived coke on AXL catalyst under sequential N_2 (to 600 °C) followed by air. Y-axis: log(Heating Rate/(°C·min^{-1})); X-axis: 1/T (K^{-1}). Activation energies from linear fits capture both inert volatilization of soft coke and oxidative combustion of hard coke.

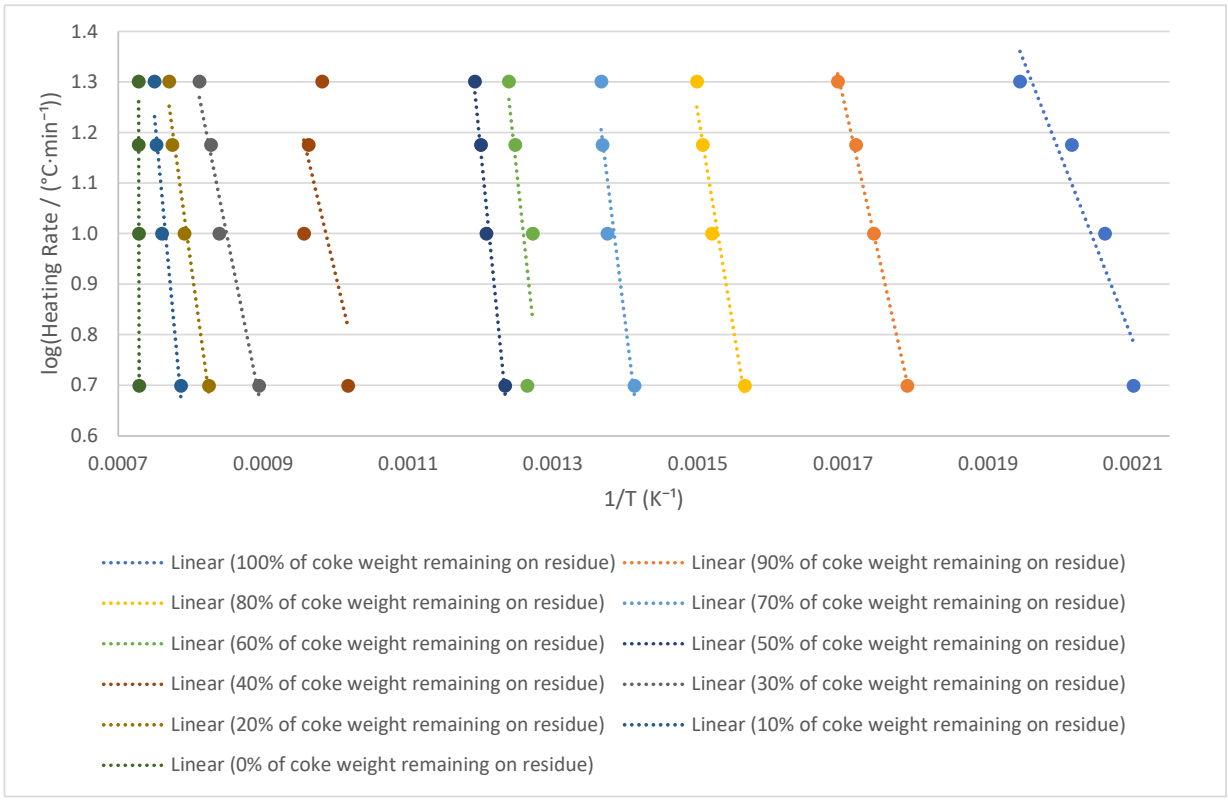

Figure A4. OFW plot for PP-derived coke on AXL catalyst under N_2 atmosphere. Y-axis: log(Heating Rate/(°C·min^{-1})); X-axis: 1/T (K^{-1}). Linear fits quantify the thermal stability of soft and hard coke fractions.

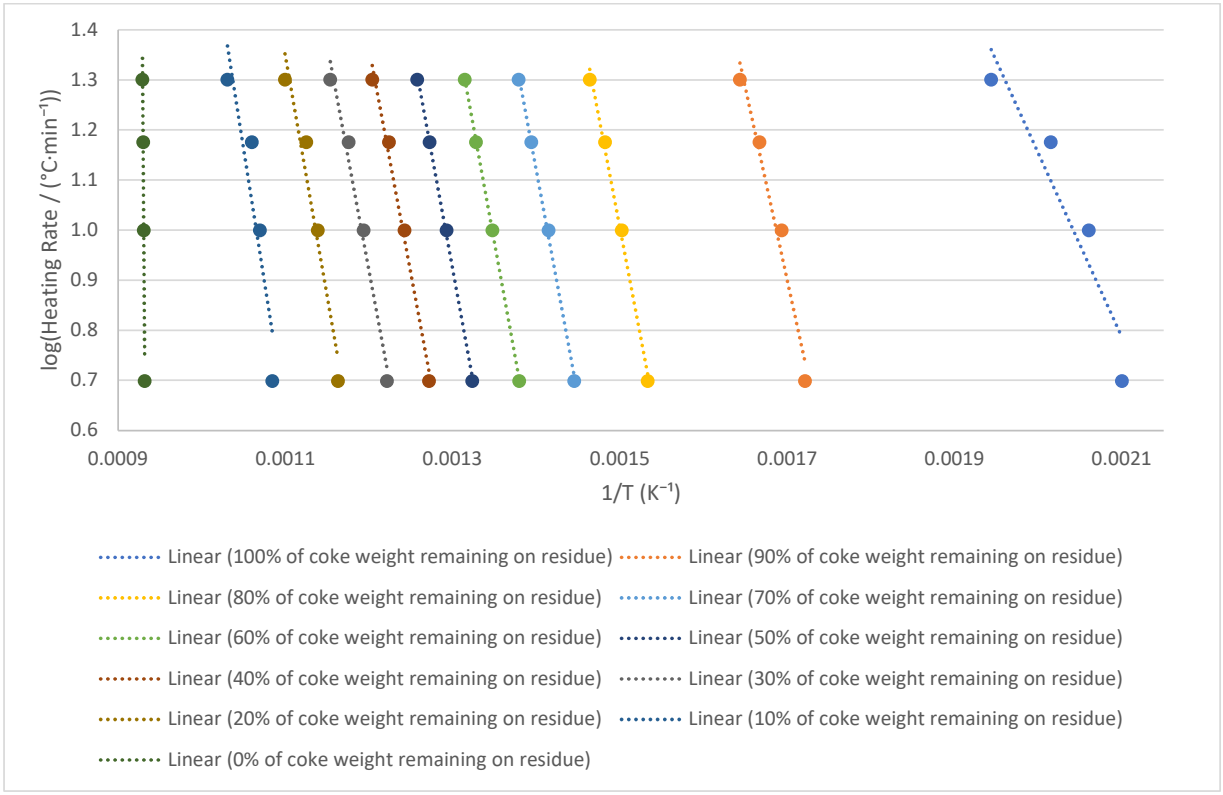

Figure A5. OFW plot for PP-derived coke on AXL catalyst under air atmosphere. Y-axis: log(Heating Rate/(°C·min^{-1})); X-axis: 1/T (K^{-1}). Linear fits reflect the activation energies of the oxidative combustion of coke fractions.

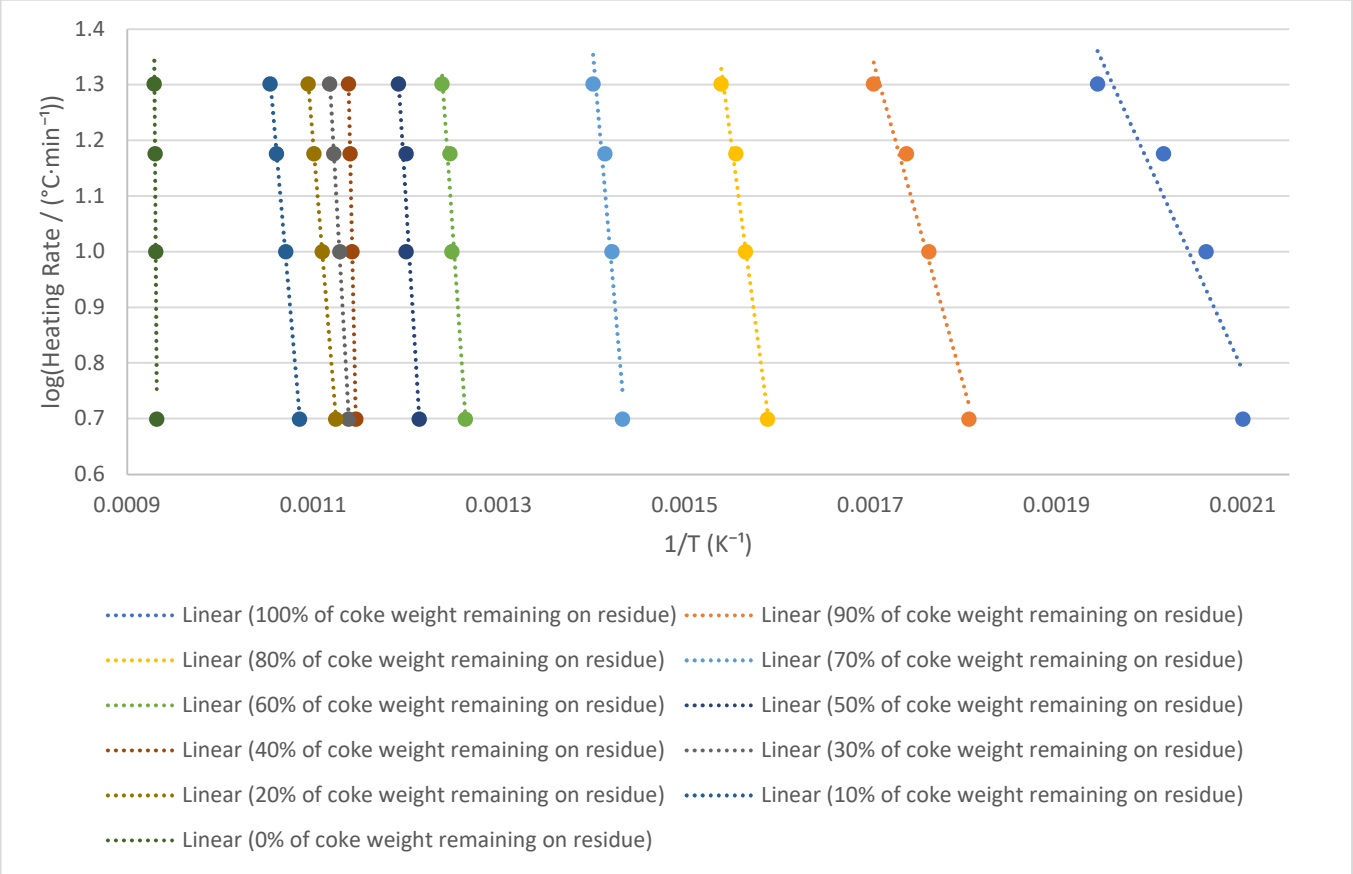

Figure A6. OFW plot for PP-derived coke on AXL catalyst under sequential N_2 (to 600 °C) followed by air. Y-axis: log(Heating Rate/(°C·min^{-1})); X-axis: 1/T (K^{-1}). Activation energies from linear fits capture both inert volatilization of soft coke and oxidative combustion of hard coke.

References

1. Brydson, J.A. *Plastics Materials*; Elsevier: Amsterdam, The Netherlands, 1999; ISBN 978-0-08-051408-6.
2. Hopewell, J.; Dvorak, R.; Kosior, E. Plastics Recycling: Challenges and Opportunities. *Philos. Trans. R. Soc. B Biol. Sci.* **2009**, *364*, 2115–2126. [CrossRef]
3. Thompson, R.C.; Moore, C.J.; vom Saal, F.S.; Swan, S.H. Plastics, the Environment and Human Health: Current Consensus and Future Trends. *Philos. Trans. R. Soc. B Biol. Sci.* **2009**, *364*, 2153–2166. [CrossRef] [PubMed]
4. Geyer, R.; Jambeck, J.R.; Law, K.L. Production, Use, and Fate of All Plastics Ever Made. *Sci. Adv.* **2017**, *3*, e1700782. [CrossRef] [PubMed]
5. Plastics Europe. *Plastics—The Facts 2022*; Plastics Europe: Brussels, Belgium, 2022; Available online: https://plasticseurope.org/knowledge-hub/plastics-the-facts-2022/ (accessed on 5 September 2025).
6. Wang, C.; Liu, Y.; Chen, W.-Q.; Zhu, B.; Qu, S.; Xu, M. Critical Review of Global Plastics Stock and Flow Data. *J. Ind. Ecol.* **2021**, *25*, 1300–1317. [CrossRef]
7. Hossain, R.; Islam, M.T.; Ghose, A.; Sahajwalla, V. Full Circle: Challenges and Prospects for Plastic Waste Management in Australia to Achieve Circular Economy. *J. Clean. Prod.* **2022**, *368*, 133127. [CrossRef]
8. Valerio, O.; Muthuraj, R.; Codou, A. Strategies for Polymer to Polymer Recycling from Waste: Current Trends and Opportunities for Improving the Circular Economy of Polymers in South America. *Curr. Opin. Green Sustain. Chem.* **2020**, *25*, 100381. [CrossRef]
9. Mihai, F.; Gündoğdu, S.; Markley, L.; Olivelli, A.; Khan, F.; Gwinnett, C.; Gutberlet, J.; Reyna, N.; Llanquileo-Melgarejo, P.; Meidiana, C.; et al. Plastic Pollution, Waste Management Issues, and Circular Economy Opportunities in Rural Communities. *Sustainability* **2021**, *14*, 20. [CrossRef]
10. Singh, P.; Sharma, V.P. Integrated Plastic Waste Management: Environmental and Improved Health Approaches. *Procedia Environ. Sci.* **2016**, *35*, 692–700. [CrossRef]
11. Davies, R. *What Is a Waste Management Hierarchy? | Axil-IS*; Axil Integrated Services: Corby, UK, 2021.
12. Babayemi, J.O.; Nnorom, I.C.; Osibanjo, O.; Weber, R. Ensuring Sustainability in Plastics Use in Africa: Consumption, Waste Generation, and Projections. *Environ. Sci. Eur.* **2019**, *31*, 60. [CrossRef]

13. Federation, B.P. Plastic Recycling. Available online: https://www.bpf.co.uk/Sustainability/Plastics_Recycling.aspx (accessed on 18 February 2025).
14. Dogu, O.; Pelucchi, M.; Van de Vijver, R.; Van Steenberge, P.H.M.; D'hooge, D.R.; Cuoci, A.; Mehl, M.; Frassoldati, A.; Faravelli, T.; Van Geem, K.M. The Chemistry of Chemical Recycling of Solid Plastic Waste via Pyrolysis and Gasification: State-of-the-Art, Challenges, and Future Directions. *Prog. Energy Combust. Sci.* **2021**, *84*, 100901. [CrossRef]
15. Davidson, M.G.; Furlong, R.A.; McManus, M.C. Developments in the Life Cycle Assessment of Chemical Recycling of Plastic Waste—A Review. *J. Clean. Prod.* **2021**, *293*, 126163. [CrossRef]
16. Solis, M.; Silveira, S. Technologies for Chemical Recycling of Household Plastics—A Technical Review and TRL Assessment. *Waste Manag.* **2020**, *105*, 128–138. [CrossRef]
17. Ragaert, K.; Delva, L.; Van Geem, K. Mechanical and Chemical Recycling of Solid Plastic Waste. *Waste Manag.* **2017**, *69*, 24–58. [CrossRef] [PubMed]
18. Sadeghbeigi, R. Chapter 4—FCC Catalysts. In *Fluid Catalytic Cracking Handbook*, 3rd ed.; Sadeghbeigi, R., Ed.; Butterworth-Heinemann: Oxford, UK, 2012; pp. 87–115. ISBN 978-0-12-386965-4.
19. Velthoen, M.E.Z.; Lucini Paioni, A.; Teune, I.E.; Baldus, M.; Weckhuysen, B.M. Matrix Effects in a Fluid Catalytic Cracking Catalyst Particle: Influence on Structure, Acidity, and Accessibility. *Chemistry* **2020**, *26*, 11995–12009. [CrossRef] [PubMed]
20. Scherzer, J. Designing FCC Catalysts with High-Silica Y Zeolites. *Appl. Catal.* **1991**, *75*, 1–32. [CrossRef]
21. Ahmad, A.; Ahmed, S.; Siddiqui, M.; Al-Shammari, A. The Investigation of Zeolite to Matrix Ratio Effect on the Performance of FCC Catalysts during Catalytic Cracking of Hydrotreated VGO. *Catalysts* **2023**, *13*, 1255. [CrossRef]
22. Elordi, G.; Olazar, M.; Castaño, P.; Artetxe, M.; Bilbao, J. Polyethylene Cracking on a Spent FCC Catalyst in a Conical Spouted Bed. *Ind. Eng. Chem. Res.* **2012**, *51*, 14008–14017. [CrossRef]
23. Vollmer, I.; Jenks, M.J.F.; Mayorga González, R.; Meirer, F.; Weckhuysen, B.M. Plastic Waste Conversion over a Refinery Waste Catalyst. *Angew. Chem. Int. Ed.* **2021**, *60*, 16101–16108. [CrossRef]
24. Manos, G.; Garforth, A.; Dwyer, J. Catalytic Degradation of High-Density Polyethylene on an Ultrastable-Y Zeolite. Nature of Initial Polymer Reactions, Pattern of Formation of Gas and Liquid Products, and Temperature Effects. *Ind. Eng. Chem. Res.* **2000**, *39*, 1203–1208. [CrossRef]
25. Gobin, K.; Manos, G. Polymer Degradation to Fuels over Microporous Catalysts as a Novel Tertiary Plastic Recycling Method. *Polym. Degrad. Stab.* **2004**, *83*, 267–279. [CrossRef]
26. Manos, G.; Garforth, A.; Dwyer, J. Catalytic Degradation of High-Density Polyethylene over Different Zeolitic Structures. *Ind. Eng. Chem. Res.* **2000**, *39*, 1198–1202. [CrossRef]
27. Manos, G.; Yusof, I.Y.; Papayannakos, N.; Gangas, N.H. Catalytic Cracking of Polyethylene over Clay Catalysts. Comparison with an Ultrastable Y Zeolite. *Ind. Eng. Chem. Res.* **2001**, *40*, 2220–2225. [CrossRef]
28. Kanattukara, B.; Singh, G.; Sarkar, P.; Chopra, A.; Singh, D.; Mondal, S.; Kapur, G.S.; Ramakumar, S. Catalyst-Mediated Pyrolysis of Waste Plastics: Tuning Yield, Composition, and Nature of Pyrolysis Oil. *Environ. Sci. Pollut. Res.* **2023**, *30*, 64994–65010. [CrossRef]
29. Duncan, J. Principles and Applications of Mechanical Thermal Analysis. In *Principles and Applications of Thermal Analysis*; John Wiley & Sons, Ltd.: Chichester, UK, 2008; pp. 119–163. ISBN 978-0-470-69770-2.
30. Corma, A.; Martínez, C.; Doskocil, E. Designing MFI-Based Catalysts with Improved Catalyst Life for C3= and C5= Oligomerization to High-Quality Liquid Fuels. *J. Catal.* **2013**, *300*, 183–196. [CrossRef]
31. Wang, B.; Manos, G. A Novel Thermogravimetric Method for Coke Precursor Characterisation. *J. Catal.* **2007**, *250*, 121–127. [CrossRef]
32. Orozco, S.; Artetxe, M.; Lopez, G.; Suarez, M.; Bilbao, J.; Olazar, M. Conversion of HDPE into Value Products by Fast Pyrolysis Using FCC Spent Catalysts in a Fountain Confined Conical Spouted Bed Reactor. *ChemSusChem* **2021**, *14*, 4291–4300. [CrossRef] [PubMed]
33. Akpanudoh, N.S.; Gobin, K.; Manos, G. Catalytic Degradation of Plastic Waste to Liquid Fuel over Commercial Cracking Catalysts: Effect of Polymer to Catalyst Ratio/Acidity Content. *J. Mol. Catal. A Chem.* **2005**, *235*, 67–73. [CrossRef]
34. Olivera, M.; Musso, M.; De León, A.; Volonterio, E.; Amaya, A.; Tancredi, N.; Bussi, J. Catalytic Assessment of Solid Materials for the Pyrolytic Conversion of Low-Density Polyethylene into Fuels. *Heliyon* **2020**, *6*, e05080. [CrossRef]
35. Omar, M.F.; Akil, H.M.; Ahmad, Z.A. Effect of Molecular Structures on Dynamic Compression Properties of Polyethylene. *Mater. Sci. Eng. A* **2012**, *538*, 125–134. [CrossRef]
36. Almeida, D.; de Fátima Marques, M. Thermal and Catalytic Pyrolysis of Plastic Waste. *Polímeros* **2016**, *26*, 44–51. [CrossRef]
37. Irawan, A.; Kurniawan, T.; Nurkholifah, N.; Melina, M.; Nandiyanto, A.; Firdaus, M.; Alwan, H.; Bindar, Y. Pyrolysis of Polyolefins into Chemicals Using Low-Cost Natural Zeolites. *Waste Biomass Valorization* **2022**, *14*, 1705–1719. [CrossRef]
38. Wang, Y.; Yan, N.; Chen, Z. Identification of Coke Species on Fe/USY Catalysts Used for Recycling Polyethylene into Fuels. *RSC Adv.* **2024**, *14*, 22056–22062. [CrossRef] [PubMed]

39. Papuga, S.; Djurdjevic, M.; Ciccioli, A.; Vecchio Ciprioti, S. Catalytic Pyrolysis of Plastic Waste and Molecular Symmetry Effects: A Review. *Symmetry* **2023**, *15*, 38. [CrossRef]
40. Maniscalco, M.; La Paglia, F.; Iannotta, P.; Caputo, G.; Scargiali, F.; Grisafi, F.; Brucato, A. Slow Pyrolysis of an LDPE/PP Mixture: Kinetics and Process Performance. *J. Energy Inst.* **2021**, *96*, 234–241. [CrossRef]
41. Zhao, D.; Wang, X.; Miller, J.; Huber, G. The Chemistry and Kinetics of Polyethylene Pyrolysis: A Process to Produce Fuels and Chemicals. *ChemSusChem* **2020**, *13*, 1764–1774. [CrossRef]
42. Das, P.; Tiwari, P. The Effect of Slow Pyrolysis on the Conversion of Packaging Waste Plastics (PE and PP) into Fuel. *Waste Manag.* **2018**, *79*, 615–624. [CrossRef]
43. Kassargy, C.; Awad, S.; Burnens, G.; Kahine, K.; Tazerout, M. Experimental Study of Catalytic Pyrolysis of Polyethylene and Polypropylene over USY Zeolite and Separation to Gasoline and Diesel-like Fuels. *J. Anal. Appl. Pyrolysis* **2017**, *127*, 31–37. [CrossRef]
44. Bagri, R.; Williams, P.T. Catalytic Pyrolysis of Polyethylene. *J. Anal. Appl. Pyrolysis* **2002**, *63*, 29–41. [CrossRef]
45. Lin, X.; Zhang, Z.; Wang, Q. Evaluation of Zeolite Catalysts on Product Distribution and Synergy during Wood-Plastic Composite Catalytic Pyrolysis. *Energy* **2019**, *189*, 116174. [CrossRef]
46. Rejman, S.; Reverdy, Z.M.; Bör, Z.; Louwen, J.N.; Rieg, C.; Dorresteijn, J.M.; van der Waal, J.-K.; Vogt, E.T.C.; Vollmer, I.; Weckhuysen, B.M. External Acidity as Performance Descriptor in Polyolefin Cracking Using Zeolite-Based Materials. *Nat. Commun.* **2025**, *16*, 2980. [CrossRef]
47. Gobin, K.; Manos, G. Thermogravimetric Study of Polymer Catalytic Degradation over Microporous Materials. *Polym. Degrad. Stab.* **2004**, *86*, 225–231. [CrossRef]
48. Muhammad, I.; Manos, G. Intensification of Co-Pyrolysis of Plastic with Biomass via Pretreatment. *Process Saf. Environ. Prot.* **2021**, *146*, 586–598. [CrossRef]
49. Muhammad, I.; Manos, G. Catalytic Copyrolysis of Heavy Oil with Polypropylene. *ACS Sustain. Chem. Eng.* **2022**, *10*, 15824–15837. [CrossRef]
50. Royo, C.; Ibarra, J.V.; Monzon, A.; Santamaria, J. Regeneration of Coked Catalysts: The Effect of Aging upon the Characteristics of the Coke Deposits. *Ind. Eng. Chem. Res.* **1994**, *33*, 2563–2570. [CrossRef]
51. Kondrasheva, N.K.; Rudko, V.A.; Ancheyta, J. Thermogravimetric Determination of the Kinetics of Petroleum Needle Coke Formation by Decantoil Thermolysis. *ACS Omega* **2020**, *5*, 29570–29576. [CrossRef]
52. Ochoa, A.; Ibarra, Á.; Bilbao, J.; Arandes, J.M.; Castaño, P. Assessment of Thermogravimetric Methods for Calculating Coke Combustion-Regeneration Kinetics of Deactivated Catalyst. *Chem. Eng. Sci.* **2017**, *171*, 459–470. [CrossRef]
53. Luo, S.; He, S.; Li, X.; Li, J.; Bi, W.; Sun, C. Combustion Kinetics of the Coke on Deactivated Dehydrogenation Catalysts. *Fuel Process. Technol.* **2015**, *129*, 156–161. [CrossRef]
54. Dubdub, I.; Al-Yaari, M. Pyrolysis of Low Density Polyethylene: Kinetic Study Using TGA Data and ANN Prediction. *Polymers* **2020**, *12*, 891. [CrossRef] [PubMed]
55. Sinfronio, F.; Santos, J.; Pereira, L.; Souza, A.; Conceição, M.; Fernandes, V., Jr.; Fonseca, V. Kinetic of Thermal Degradation of Low-Density and High-Density Polyethylene by Non-Isothermal Thermogravimetry. *J. Therm. Anal. Calorim.* **2005**, *79*, 393–399. [CrossRef]
56. Al-Shathr, A.; Al-Zaidi, B.Y.; Shehab, A.K.; Shakoor, Z.M.; Aal-Kaeb, S.; Gomez, L.Q.; Majdi, H.S.; Al-Shafei, E.N.; AbdulRazak, A.A.; McGregor, J. Experimental and Kinetic Studies of the Advantages of Coke Accumulation over Beta and Mordenite Catalysts According to the Pore Mouth Catalysis Hypothesis. *Catal. Commun.* **2023**, *181*, 106718. [CrossRef]
57. Goonvean Fibres Ltd. Polypropylene Fibre. Available online: https://goonveanfibres.com/products-services/polypropylene/ (accessed on 5 September 2025).
58. Goonvean Fibres Ltd. Polyethylene Fibre & Powder. Available online: https://goonveanfibres.com/products-services/polyethylene/ (accessed on 5 September 2025).
59. Federation, B.P. Polyethylene (Low Density) LDPE, LLDPE. Available online: https://www.bpf.co.uk/plastipedia/polymers/LDPE.aspx (accessed on 29 April 2025).
60. Digi-Sense TC9600 Benchtop Temperature Controller with USB Output, for Thermocouple, RTD, or Thermistors; 230 VAC from Cole-Parmer United Kingdom. Available online: https://www.coleparmer.co.uk/i/digi-sense-tc9600-benchtop-temperature-controller-with-usb-output-for-thermocouple-rtd-or-thermistors-230-vac/8980014 (accessed on 25 February 2025).
61. PicoScope Oscilloscope Software and PicoLog Data Logging Software. Available online: https://www.picotech.com/downloads (accessed on 25 February 2025).
62. Ozawa, T. A New Method of Analyzing Thermogravimetric Data. *Bull. Chem. Soc. Jpn.* **1965**, *38*, 1881–1886. [CrossRef]
63. Doyle, C.D. Kinetic Analysis of Thermogravimetric Data. *J. Appl. Polym. Sci.* **1961**, *5*, 285–292. [CrossRef]

64. Aboulkas, A.; El Harfi, K.; El Bouadili, A. Thermal Degradation Behaviors of Polyethylene and Polypropylene. Part I: Pyrolysis Kinetics and Mechanisms. *Energy Convers. Manag.* **2010**, *51*, 1363–1369. [CrossRef]
65. Xu, F.; Wang, B.; Yang, D.; Hao, J.; Qiao, Y.; Tian, Y. Thermal Degradation of Typical Plastics under High Heating Rate Conditions by TG-FTIR: Pyrolysis Behaviors and Kinetic Analysis. *Energy Convers. Manag.* **2018**, *171*, 1106–1115. [CrossRef]